The Thesis Committee for Rogelio Ortiz
Certifies that this is the approved version of the following thesis:

Fire Retardant Polyamide 11 Nanocomposites/Elastomer Blends for Selective Laser Sintering

APPROVED BY
SUPERVISING COMMITTEE:

Supervisor: _____
David L. Bourell

Co-Supervisor: _____
Joseph H. Koo

Fire Retardant Polyamide 11 Nanocomposites/Elastomer Blends for Selective Laser Sintering

by

Rogelio Ortiz, B.S.

Thesis

Presented to the Faculty of the Graduate School of

The University of Texas at Austin

in Partial Fulfillment

of the Requirements

for the Degree of

Master of Science in Engineering

The University of Texas at Austin

May 2016

To my teachers, *for their guidance and knowledge instilled in me*

To my siblings, *for always being there for me*

and of course

To my parents, *for believing in me and giving me the courage and motivation to never give up*

Acknowledgements

Today, as my graduate studies come to an end, I look back upon all those memories and new friends I made during my last two years of my life. I look back upon all the great things I learned and accomplished, and of one thing I am certain. It is because of people that crossed my path during this stage of my life that I was able to accomplish what I did today. And because of that, I will forever be grateful.

I would like to thank my wonderful advisor, Dr. Joseph H. Koo, for his guidance and support throughout my graduate studies. It was an honor working with such a wonderful person. Without his guidance and financial support, this research would have never been possible. I would also like to thank Dr. David L. Bourell for his feedback and for taking the time to read this thesis. Dr. Wei Li for believing in me and always being there for me whenever I needed something. My lab mate, Hao Wu, for training me to use all the equipment necessary for this research and answering all of my questions. Dr. Mourad Krifa for allowing me to use his equipment. I would also like to thank all the students from Dr. Koo's research group who helped in the progress of this research. Special thanks to KAI, LLC for their financial support and Texas Research Institute Austin, Inc. for giving me the opportunity to work and learn many things.

Second, a good amount of work for this research involved the use of an injection molding machine at Texas State University-San Marcos. For this reason, I want to thank Dr. Tate for allowing me to use his equipment and all of his students at Texas State

University for being very supportive and helpful in getting my test specimens done every time I went there.

Lastly, I would like to thank my siblings for their love and giving me the motivation to continue with my education. I would also like to thank my beautiful girlfriend, Brenda, for putting up with me all this time. I would like to express my sincere gratitude and thanks to my parents. Without their hard work, dedication, and sacrifices, I would not be standing where I am today. They have taught me that through hard work and willingness to succeed in life, everything is possible.

ROGELIO ORTIZ

The University of Texas at Austin

May 2016

Abstract

Fire Retardant Polyamide 11 Nanocomposites/Elastomer Blends for Selective Laser Sintering

Rogelio Ortiz, M.S.E.

The University of Texas at Austin, 2016

Supervisor: David L. Bourell

Co-Supervisor: Joseph H. Koo

Additive manufacturing (AM) had previously been used solely for prototyping and visualization purposes, but in recent years, this technique has shifted to the idea of producing end-use parts. This has already been successfully done in some areas via selective laser sintering (SLS). Unfortunately, current polymeric materials for processing via SLS do not meet the requirements of the majority of commercial applications. Hence, this thesis presents efforts to develop a multifunctional polyamide 11 (PA11) polymer with enhanced thermal, mechanical, and flammability properties for SLS through the use of nanotechnology.

Table of Contents

List of Tables

List of Figures

CHAPTER 1: INTRODUCTION

1.1 Additive Manufacturing

Recently, additive manufacturing (AM) has gained unprecedented attention from many researchers around the world. AM refers to the different processes used to fabricate three-dimensional objects directly from digital models through an additive process by selectively curing, depositing, or consolidating materials in successive layers of polymers, ceramics, or metals [1]. Originally, AM had been used to fabricate suitable prototypes for visualization purposes. However, in recent years, additive techniques are increasingly being considered for the production of end-use parts in the automotive, medical, and aerospace industries because of their capabilities to manufacture more geometrically complex parts than traditional processes [2].

Currently, there is variety of AM processes available, such as stereolithography (SLA), fused deposition modeling (FDM), three-dimensional printing (3DP), selective laser sintering (SLS), and others [1]. When compared to additive manufacturing processes suitable for making end-use parts, SLS is significantly relatively inexpensive to operate. Moreover, due to its advantage to fabricate parts from a wide range of commercially available materials, especially polymers, SLS is a great process to use for AM and is the focus of this thesis [3].

1.2 Selective Laser Sintering

SLS was developed by Carl Deckard for his Ph.D. research at the University of Texas at Austin, and it was patented in 1989. This technique uses a laser beam to fuse particles of plastic, metal, or glass powders into a desired three-dimensional shape. The

process builds an object by analyzing a three-dimensional model of the object, then breaking it down into cross sections of small thickness typically less than 0.25 mm (Figure 1). These cross sections are then used as layers of a part build. A very fine powder is distributed onto a central platform using a feed and roller system. Once the powder is deposited, a laser is used to sinter it together into contours of the pre-established layers. Upon completion, the layer is lowered, covered by a new layer of powder, and the process is repeated until the cross sections of the entire model have been finished [3].

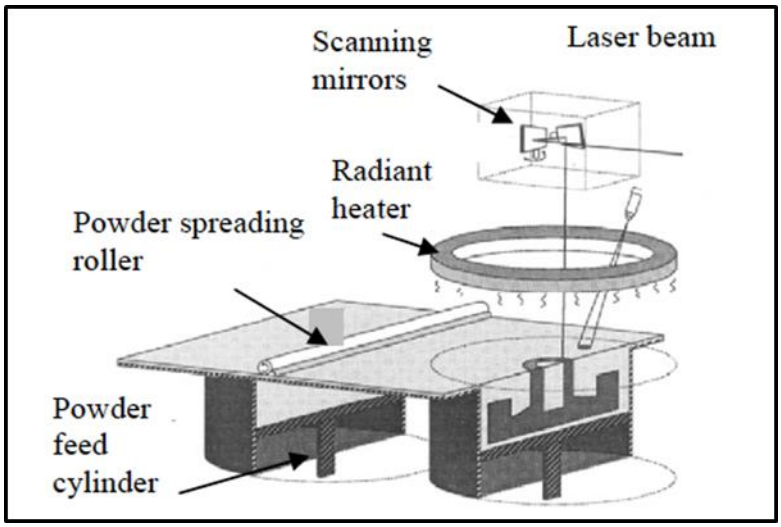

Figure 1: Schematic of selective laser sintering process [4].

1.2.1 SLS Build Parameters

In this procedure, several key machine and build parameters affect the quality of a part. The primary parameter involved is the laser energy transmitted into the build material, which is derived from the laser power, the scan speed, and the scan spacing. The laser power is the energy directed onto the part bed as opposed to the total wattage

input into the laser. The scan speed is the velocity at which the laser moves across the part profile. The scan spacing is the physical gap between each scanning sweep [5]. Energy density can be defined by these three factors using the following equation:

$$[Energy\ density] = \frac{[Laser\ Power]}{[Scan\ Speed][Scan\ Spacing]} \quad (1)$$

Energy densities that are excessive will typically result in poor dimensional tolerances, which in turn can cause issues during the mechanical operations inside the build chamber. Energy densities that are too low will cause improper particle adhesion and eventual disintegration of the parts [6].

Another important parameter involved in this process is the build chamber temperature control. With a standard SLS machine, the operator controls the part bed and feed bin temperatures. In order to produce successful parts, these temperatures must be carefully maintained within the build medium's tolerable range. Failure to properly pre-heat the powder reservoirs or the workspace can result in poor adhesion. Over-heating results in the opposite effect by over-sintering more material than is desired and producing parts with poor dimensional tolerances. Additionally, if heat distribution of the layers is improperly regulated, curling, a phenomenon in which the gradient of layers undergoes irregular thermal contraction and physically bends the part structure may occur. Often, this will cause a build to be terminated if it occurs during the procedure [6]. Furthermore, curling can also occur post-procedure if the build is cooled too quickly, which typically results in the delamination of a part (Figure 2).

Figure 2: Top (left) and cross-sectional view (right) of tensile specimen subjected to curling [7].

1.2.2 SLS LIMITATIONS

Although only 27 years since it was patented, SLS is still at its infancy and many limitations exist. For instance, the manufacturing of parts is relatively slow, there is limited object size, materials cost is high, and limited availability of materials from which to manufacture end-use parts that meet the requirements of the majority of commercial applications [8]. In the past few years, researchers are addressing this area and have focused on gaining a better understanding of the processing of polymers by SLS to develop new polymers that can successfully be processed for end-use [9]. These technological advancements show promise and indicate that SLS will thrive globally in the development of prototypes and finished parts [10].

1.3 Implementation of Polymer Nanocomposites in Selective Laser Sintering Literature Review

Polymer nanocomposites are of considerable importance for SLS since a relatively small amount of nanoparticles can affect the properties of the polymer. Numerous attempts have been reported to improve the mechanical and physical properties of polymeric laser sintered parts by reinforcing them with nano-sized fillers, such as nanoclay (NC), carbon nanofibers (CNFs), nanosilica (NS), nano-Al_2O_3, multi-walled nanotubes (MWNTs), and other nanoparticles [9]. Besides mechanical and physical properties improvements, researchers have used nanoparticles to enhance other properties, such as electrical, thermal conductivity, heat resistance, and reduced flammability with promising results. As research on polymer nanocomposites with polymers, such as Nylon 6 (PA6), Nylon 11 (PA11), and Nylon 12 (PA12) continues, improvements in processing and characterization have yielded better mechanical, electrical, thermal, and reduced flammability properties for SLS products. This review will describe and analyze previous research conducted in polymer nanocomposites to improve these properties for their implementation in SLS. It is important to note that the studies mentioned here are preliminary and future studies will be carried out as the material development for laser sintering progresses. Up to this date, most of the published work focuses on polyamide-based materials PA11, and PA12. Consequently, for the purpose of this study, only the studies mentioned here are focused on PA11.

PA11 is a thermoplastic that is widely used in SLS. It has good elongation, good abrasion resistance, and good specific strength, but lacks high heat resistance and flame

retardancy. These latter shortcomings are required properties for performance driven applications. The addition of nanomaterials to PA11 can enhance these properties to a desired level and may result in additional market opportunities for PA11 manufacturers [11].

Chung [12] mechanically mixed neat polymer powders with filler particles to prepare a PA11/NS nanocomposite powder. The results show that NS was not successfully dispersed in the SLS parts. It was concluded that because of the different densities and polarities of the two powdered materials, it was difficult to uniformly mix them and achieve a homogeneous distribution in the SLS parts. Lao et al. [13, 14] have shown that PA11/NC and PA11/CNFs exhibited better flammability and thermal properties than neat PA11. However, the elongation at break was decreased by both the NC and CNFs. They successfully fabricated SLS parts with these materials, but the parts did not exhibit the optimal flame retardant properties for the intended application [14].

Lao et al. [15] expanded these previous studies to include the use of MWNTs in the PA11 polymer matrix. They compounded separately via twin-screw extrusion a total of five formulations of PA11/MWNT nanocomposites as well as another three formulations of PA11/MWNT nanocomposites fabricated by mixing PA11 powder with pulverized MWNT using Thinky mixer. For the twin-screw extrusion, the transmission electron microscope (TEM) results showed a satisfactory dispersion of MWNTs in the PA11 matrix. It was also shown that the MWNTs improved the mechanical properties, with the exception of elongation at break, as well as thermal stability and electrical conductivity of PA11. In this study, at 60% mass loss decomposition, the temperature of

neat PA11 is about 450°C whereas the mass loss decomposition temperature of PA11 with 20 wt% MWNT is about 500°C. This shows that the addition of higher concentrations of MWNT significantly increased the mass loss decomposition temperature and achieved better thermal stability. However, all five formulations processed via twin-extrusion failed the UL 94 flammability test. For the PA11-MWNT formulations fabricated by mixing PA11 powder with pulverized MWNT using a Thinky mixer, the dispersion of the nanoparticles was examined via scanning electron microscopy (SEM), which showed MWNT clusters attached to the PA11 particles. However, it was well dispersed evenly on the surface. At 60% mass loss, film A mass loss decomposition temperature was at about 470°C whereas PA11 with 20% MWNT mass loss decomposition temperature was at about 500°C. Comparing the two sets of MWNT, the set processed by twin-screw extrusion was better.

In a more recent study of Yuan et al [15], MWNT additives were incorporated into PA11 and showed a very good dispersion with no agglomerates. There was an improvement in thermal conductivity by two or three orders of magnitude to that of neat PA11 as well as an improvement in electrical conductivity just as shown by Lao et al. From these studies, it is clear that MWNTs in PA11 improves the mechanical properties, except for elongation at break, flammability, electrical, and thermal properties. This was a preliminary study to determine how thermal and electrical conductivities behavior of PA11 polymer can be improved. They suggested that further experimentation is necessary to examine how well PA11 will perform under SLS conditions [16].

Chen et al. [17] and Gaikwad et al. [18] modified PA11 by using nanographene platelets (NGPs). NGPs have excellent electrical properties, thermal, and mechanical properties. Chen et al. [17] added NGPs to PA11 powder via powder-powder mixing. Results confirm that there was not a good dispersion. A slight decrease in thermal stability and no improvement in electrical conductivity were noticed. On the other hand, Gaikwad et al. [18] blended PA11 with NGPs via industrial size co-rotating twin-screw extrusion. SEM analysis demonstrated that there was a good uniform dispersion and exfoliation of NGPs within the PA11 matrix. The results show that the tensile strength at 1 wt% was better than neat PA11, but it decreased as the wt% increased. The opposite happened with flexural strength. At 1 wt%, the flexural strength of neat PA11 was higher, but as the wt% of NGP increased, the flexural strength actually became significantly better than neat PA11. Furthermore, because of the high shear that occurs when mixing the NGPs into the polymer matrix by the twin-screw extrusion, the NGPs break down, which in return decreases the elongation at break. There was an increase in thermal stability as NGP wt% increased. There was also a slight but insignificant improvement in flammability compared to neat PA11. They suggested that future work involves counter rotating twin-screw extrusion with less high shear action to achieve improved electrical and mechanical properties.

Lao et al. [11] have shown that low amounts of nanoparticles enhance some of the mechanical properties, but lack fire retardancy when compared to those flame retardant thermoplastics with conventional fire retardant additives (FR). Lao et al. [19] added NC and CNFs with conventional intumescent FR additives to polyamide 11 to study the

flammability properties. It was shown that there was a good dispersion of NC and CNFs in the PA11 matrix. It was also shown that systems with a combination of both nanoparticles and FR additive had better thermal stability in comparison to those systems with either the FR additive or the nanoparticles. A synergism was established in terms of thermal and flammability properties that occur between the nanoparticles and the intumescent FR additive.

Johnson et al. [20] prepared specimens of PA11 with different loadings of intumescent FR additives, NC, and CNFs via the twin screw extrusion technique. The modified PA11 had lower tensile strength compared to the neat PA11. However, all modified PA11 had superior modulus compared to neat PA11 where higher concentrations of NC and CNFs in the polymer resulted in higher tensile modulus. Just as in Lao et al. [19], PA11 with a combination of FR additive and a nanomaterial exhibited better tensile strength and modulus in comparison to specimens with a single nanomaterial. This was not the case with elongation at break. It was concluded that there are synergistic effects of multiple nanoparticles with a conventional FR additive. It was observed that a synergistic effect between NC, CNFs, and FR exists where only 15 % of FR additives, 2.5 % NC, and 2.5 % CNFs are needed to achieve a UL 94 V-0 rating as compared to at least 20 % of FR additives with 5% of CNFs or 7.5 % NC if used individually in the PA11 matrix.

In another study, Lao et al. [21] used twin-screw extrusion to disperse low concentrations of NC, CNFs, and NSs to melt-blended polyamide 11. Intumescent FR additives were compounded via twin-screw extrusion as well. The combination of FR and

nanoparticles had a good effect on PA11 blends as it increased their decomposition temperatures compared to only using FR additives.

Koo et al. [13] created polyamide 11 nanocomposites via twin-screw extrusion by using polyamide 11 molding polymer pellets and three types of nanoparticles: chemically modified NC, surface modified NS, and CNFs. The TEM showed that NC and CNFs in the polyamide 11 were well dispersed whereas NS was not. The addition of NC and CNFs enhanced the FR properties of PA11. There was a decrease in the elongation at break for PA11 modified by NC and CNFs. The authors were able to successfully fabricate SLS parts.

Lao et al extended their studies [19, 21] to further enhance the mechanical properties of PA11/FR nanocomposites by using different FR additives while maintaining the same amount of NC and CNFs. Different weight loadings of NC, CNFs, and the newly selected intumescent FR additives were melt-blended with polyamide 11 via twin-screw extrusion. A uniform dispersion for both NC and CNFs was observed for the polyamide 11 polymer systems. When comparing the results to their previous studies, they found that the new FR additive used in this study performed better with the NC, whereas the FR additive used by the authors in [19] performed better with the CNFs in regards to mechanical properties. For thermal stability, the FR additive used in reference [19] performed better with NC whereas the new FR additive used in [21] performed better with CNFs.

Lao et al. [22] blended different combinations of PA11, NC, CNFs and three different intumescent FR additives via twin-screw extrusion. This study is an expansion

of Lao et al.'s [21, 23]. Lao et al. [22], showed that the thermal stability of the PA11 was significantly enhanced by both NC and CNFs. Also, the decomposition temperatures of all FR/NP-reinforced PA11 blends were higher compared to those with NP only. From this study, it was concluded that there is superior thermal and reduced flammability property characteristics due to an improved synergism between FR additives and nanoparticles.

Hao et al. [24] studied PA11, FR, and halloysite nanotubes (HNTs) nanocomposites via twin-screw extrusion melt compounding. There was a uniform dispersion of HNTs in the PA11 matrix as shown by the TEM micrographs. There was an improvement in mechanical strength, stiffness, and toughness by modifying PA11 with HNTs. In addition, the formula with 25% FR and 2.5 HNTs possessed lower additives and the best elongation at break of 10.22%. The FR and HNTs proved to be effective in reducing the thermal combustion activity. The results show that overall effectiveness of PA11/FR/HNT nanocomposites to be valuable for high-performance compositions for the SLS process. They have proposed the addition of an elastomer component in the PA11/FR/HNT nanocomposites to increase the elongation at break for their future work.

Ong et al. [7] successfully built PA11/MWNT test SLS specimens. From this study, it was concluded that the SLS nanocomposite parts of PA11/MWNT achieved enhanced electrical conductivity when compared to neat PA11 with minimal losses in material strength.

Table 1 gives a summary of the nano-reinforced PA11 formulations previously discussed. This table describes whether or not a good dispersion was achieved, what

material properties were analyzed, and whether or not there was a significant improvement in the thermal, flammability, mechanical, and electrical properties.

Table 1: Summary for PA11 modified formulations discussed in literature review

Formulation	Good Dispersion?	Thermal Properties	Flammability Properties	Mechanical Properties	Electrical Properties
Nanosilica (NS)	No [12, 13, 21]	Not enhanced [21]	Enhanced [21]	N/A	N/A
Nanoclay (NC)	Yes [13, 21]	Enhanced [13, 21]	Enhanced [13, 21]	Elongation decreased [13]	N/A
Multi-wall carbon nanotubes (MWNTs)	Yes [16]	Enhanced [7, 16]	Not enhanced [7]	Elongation decreased [7]	Enhanced [7, 16]
Nanographene (NGP)	No [17] Yes [18]	Not enhanced [17] Enhanced [7, 18]	No significant change [18]	Better tensile and flexural modulus [18]	Enhanced [7, 18]
Carbon nanofibers (CNFs)	Yes [13, 21]	Slightly enhanced [13, 21]	Enhanced [13, 21]	Elongation decreased [13]	N/A
Nano-alumina	Yes [11]	Enhanced [11]	Enhanced [11]	N/A	N/A
Halloysite (HNT)/FR	Yes [24]	Enhanced [24]	Enhanced [24]	Elongation decreased [24]	N/A

Table 1, continued.

NC/FR	Yes [19, 21, 22, 25]	Enhanced [19, 21, 22, 25]	Enhanced [19, 21, 22, 25]	N/A	N/A
CNFs/FR	Yes [19, 21, 22, 25]	Enhanced [19, 21, 22, 25]	Enhanced [19, 21, 22, 25]	N/A	N/A
NC/CNFs/FR	N/A	N/A	Enhanced [20]	Elongation decreased [20]	N/A

1.4 Motivation and Statement of Problem

Models processed by SLS were predominantly used for prototyping and visualization, and they were only required to possess sufficient mechanical integrity and surface quality for demonstration purposes. As a consequence, there was no need to know the material's mechanical properties between parts and different materials from which to manufacture the models. However, as SLS becomes more popular to manufacture end-use parts, these factors are becoming very important, and current materials used in SLS do not meet the requirements of the majority of commercial applications [9]. Hence, there is a need to develop new materials other than the ones currently available. PA11 is one of the most widely used polymers in SLS and has succeeded in some areas, such as producing air ducting systems for F18 Fighter jets as well as producing hearing aid shells.

Although some great advancement has been made in these areas, PA11 is very flammable, which limits its applications [20].

The flammability of polymers can substantially be reduced by adding large amounts of FR additives, such as inorganic metal oxides and hydroxides or halogens with or without phosphorous and nitrogen-containing materials, Unfortunately in most cases, the addition of FR additives has a negative effect on the polymer as they reduce some of its mechanical properties, such as toughness and elongation at break, and release smoke and toxic emissions when burned, which is a critical safety issue [19].

These material restrictions are one of the main drawbacks to the advancement of the SLS technology. As it was discussed earlier in the literature review section, studies have shown that this flammability issue can be resolved by adding small amounts of nanoparticles and reducing the amount of FR additives in the polymer matrix. The above strategy yields the same results as well as enhanced mechanical properties, such as higher tensile strength and modulus, and higher heat deflection temperature [19, 21]. Research in the field of polymer nanocomposites for SLS has hence expanded dramatically in the recent years. Typically, in this process, polymers are infused with nanoadditives in the nanometer (10^{-9} meter) scale to improve the overall strength, stiffness, thermal conductivity, fire retardancy, and/or other properties [6, 26]. The reinforcement of the polymer only requires a low loading [27].

Even though it has been shown that the addition of both FR additives and nanoparticles into the polymer matrix of PA11 can reduce its flammability property, the elongation at break of these new materials is considerable poor when compared to neat

PA11. There has been, however, some mechanical property data reported for PA6 reinforced with FR additives and thermoplastic elastomers, which shows that the elastomers effectively recovered elongation at break back to over 100% [28].

Hence, for this research, a formulation with improved flammability properties as well as improved mechanical properties, but more specifically, improved elongation at break is sought. To achieve this, formulations containing multi-components of NC, MWNTs, FR additive, and an elastomer were blended together with PA11 to investigate. The purpose is to improve the flammability properties while maintaining acceptable levels of mechanical properties gained by adding an elastomer component.

In order to develop the optimal formulation to meet these requirements, specimens for testing were first made via injection molding since it is considerably faster and cheaper than making the same specimens via SLS. After finding the best formulation, about 80 pounds of this formulation will be compounded using an industrial twin-screw extruder, and then the extruded mixture will be cryogenically grinded into a fine powder to use in SLS. Finally, parameter optimization in the SLS machine will be carried out to find the optimal build chamber temperatures, scan speed, laser power, and scan spacing by making density cubes and tensile specimens. For this study, only injection molding specimens were made, tested, and analyzed.

CHAPTER 2: PROCESSING OF POLYMER NANOCOMPOSITE/ELASTOMER BLENDS FOR INJECTION MOLDING

2.1 Materials

Based on the previous studies discussed in the literature review section, the following materials were selected as candidates for PA11 polymer nanocomposite formulations with improved elongation at break and flammability properties.

2.1.1 POLYMER RESIN

The base polymer used in this study is Rilsan® PCG LV polyamide 11 manufactured by Arkema Inc. Technical Polymers (Lacq, France). PA11 is a high performance polymer of 100% renewable origin with good abrasion resistance, crack propagation, heat resistance, ductility, and easy processing. PA11 has a melting temperature of 189ºC.

A copolymer, Kraton FG1901 G (K), was provided from Kraton Polymers Inc. (Houston, TX, USA) as a dusted pellet. K is a clear triblock copolymer based on styrene and ethylene/butylene with a polystyrene content of 30% and has and elongation at break of 500%.

2.1.2 NANOPARTICLES

Two types of nanoparticles were used in this study: Cloisite® 30B nanoclay (NC) and Baytubes C 70 P multi-walled carbon nanotubes (MWNTs). The addition of these two nanoparticles into the polymer matrix will reinforce the material in the nanoscale as well as enhance the dimensional stability and mechanical properties. Thermosetting and

thermoplastic nanomodification is well documented by Koo [29]. In order to achieve the potential improvements by the addition of the nanoparticles in the polymer matrix, usually, the nanoparticles require a uniform dispersion, which is achieved by optimized processing.

Cloisite® 30B was provided by Southern Clay Products. Cloisite® is often used as an additive for plastics to improve various plastic physical properties, such as heat deflection temperature, coefficient of linear thermal expansion, and to form a barrier.

Baytubes C70 P was provided by Bayer MaterialScience. This nanomaterial has improved dispensability, which makes them highly suitable for mechanically sensitive polymers.

2.1.3 FIRE RETARDANT ADDITIVE

The FR additive used for this study is Exolit® OP1312 provided by Clariant International Ltd. (Germany). This white powder intumescent FR additive is based on organic phosphinates, and it contains phosphorus and other proprietary FR components. It is not halogenated and has good thermal stability. A thermoplastic polymer with Exolit® OP1312, when exposed to a flame, foams and crosslinks to form a stable char that acts as a barrier.

2.2 Processing and Specimens Preparation

Throughout this research, a total of three sets of six formulations were melt-blended with different concentrations of FR, K, NC, and PA11 as shown in Table 2 to 4 using a Thermo Scientific Process 11 Parallel Twin Screw Extruder. The specific operating conditions for each of the melt-blended batches are shown in the following

tables. PA11 was dried at 80ºC for 24 hours prior to processing. The FR additive, K, NC, and MWNT were used as received. To ensure a homogenous dispersion, each formulation was pre-mixed by physical stir mixing prior to melt-compounding. The extruded formulations were made into small pellets and air cooled and dried at 80ºC for 24 hours before injection-molding. Table 2 to 4 show the processing conditions for each set for this study, which include the feeding rate of the material, the twin-screw speed, the temperature between the different sections in the twin screw, the Mini-Jector temperature at three different locations, and the mold temperature.

Table 2: Processing conditions for the PA11/FR/K matrix

Processing Conditions					
Feeding rate (gm/h)	200				
Screw speed (rpm)	220				
Twin screw temperature (ºC)	195	195	195	195	195
Mini-Jector temperature (ºC)	195		207		216
Mold temperature (ºC)	90				

Table 3: Processing conditions for the PA11/FR/K/NC matrix

Processing Conditions					
Feeding rate (gm/h)	200				
Screw speed (rpm)	195				
Twin screw temperature (ºC)	195	195	195	195	195
Mini-Jector temperature (ºC)	187		195		201
Mold temperature (ºC)	90				

Table 4: Processing conditions for PA11/FR/K/NC/MWNT matrix

Processing Conditions					
Feeding rate (gm/h)	200				
Screw speed (rpm)	150				
Twin screw temperature (ºC)	210	210	210	210	210
Mini-Jector temperature (ºC)	190		215		218
Mold temperature (ºC)	90				

CHAPTER 3: CHARACTERIZATION OF EXTRUSION-INJECTION MOLDED POLYMER NANOCOMPOSITE/ELASTOMER BLENDS

3.1 Thermal Stability

Thermal stability is a substance's resistance to permanent property changes caused solely by heat. Thermogravimetric analysis (TGA) is a commonly used metric to assess thermal stability of polymers namely decomposition temperature. Thermal decomposition of each polymer blend was assessed by a TGA-50 from Shimadzu Scientific Instruments, which measures the mass of the sample as a function of temperature in a closed nitrogen environment. The samples were heated in a nitrogen environment from room temperature to 1000°C at a heating rate of 10°C/min. The nitrogen flow was 20ml/min. A single TGA test was performed on each blend and was used to determine the 10% and 50% mass loss decomposition temperatures, $T_{10\%}$ and $T_{50\%}$, respectively.

3.2 Flammability

Different test protocols and methods, such as micro-scale combustion calorimetry (MCC) and UL 94 (The Standard for Flammability of Plastic Materials for Parts in Devices and Appliances) have been developed to quantify the 'degree of difficulty' required to initiate and perpetuate combustion in plastics.

3.2.1 MICRO-SCALE COMBUSTION CALORIMETRY (MCC)

A Micro-scale Combustion Calorimeter (MCC2, Govmark, Inc.) was used to measure the thermal combustion properties according to ASTM D7309-2007. The combustor temperature was held constant at 900°C and the heating rate of the pyrolysis

was 1°C/sec. The percentage of oxygen concentration was measured to calculate the heat release.

3.2.2 UL 94

UL 94 is a standard, small scale, flame test for flammability of plastics materials, which determines the material's tendency to either self-extinguish or to spread the flame once the specimen has been ignited. This test is a preliminary indication of a plastic's acceptability for its use as a component of a device or appliance. It is important to note that UL 94 does not represent the material's hazards under actual fire condition, but it is simply a preliminary step towards obtaining recognition under the 'Plastics Recognized Component Directory.' There are three ratings, V-2, V-1, and V-0, where V-0 is the best. These ratings indicate that the material was tested in a vertical position, the time it took to self-extinguish, and whether or not the test specimen dripped flaming particles that ignited a cotton indicator below the sample. The test setup is shown in Figure 3. For this study, the UL 94 testing requirements and procedures were followed even though our lab is not officially certified for UL 94 testing. As a consequence, the results serve only as a screening tool. The materials were conditioned for 48 hours at 25°C and 50% relative to humidity before testing. A total of five ½" x 5" specimens were tested for each blend. The specimen is held vertically at one end and cotton is placed underneath. The other end of the specimen is exposed to a burner flame for 10 seconds and the time it takes to self-extinguish is recorded. The specimen is exposed to the flame for another 10 seconds and the time it takes to self-extinguish is recorded again and whether or not the material dripped and burned the cotton underneath [30].

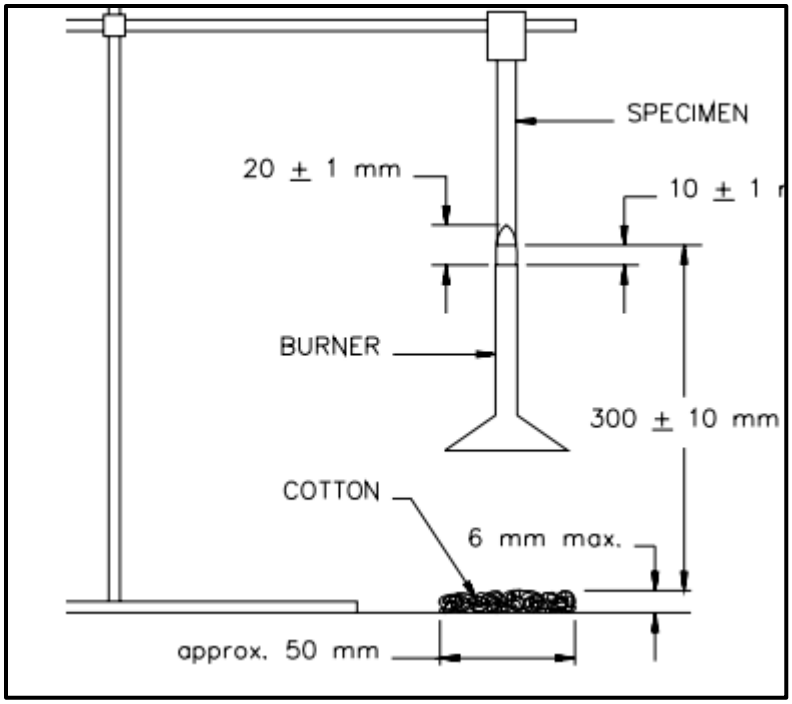

Figure 3: Vertical burning test setup [30].

3.3 Tension Testing

The tension tests were performed using an Instron Tension Tester with model number 5966. The crosshead speed was 5 mm/min and the gauge length was 115 mm. Prior to testing, the samples were conditioned at 25°C and 50% relative humidity for 48 hours. The average values and standard deviation (SD) of the tensile properties were calculated by testing 5 specimens for each formulation.

3.4 Morphological Microstructural Analysis

The cross-sections of PA11 nanocomposites were subjected to an SEM to investigate the material morphology. The fractured surface of the post-test tensile specimens of some of the formulations with the best flammability properties are analyzed

to gain a better understanding of how the additives affect the structure and properties of the nanocomposite material. In the same way, another microstructural analysis will be conducted on post-test UL 94 specimens to gain a better understanding of the protective mechanism.

CHAPTER 4: RESULTS AND DISCUSSION

4.1 Results and Discussion for First Masterbatch

Previous studies by Lao et al. have shown that only 20% of FR additive achieves desirable flammability properties, but the elongation at break property significantly decreases [11, 15, 19, 21, 22, 23, 25]. It was suggested by Hao et al. that the addition of an elastomer might help to bring back some of the elongation at break [24]. Wu et al. successfully reinforced PA6 with the same FR additive and thermoplastic elastomer used in his study showing that the elastomer effectively recovered the elongation at break back to over 100% [28]. It was of interest to see how PA11 will interact with the FR and the elastomer. For our first study, a total of six formulations were melt-blended with a constant concentration of 20% of FR additive and different loadings of elastomer as shown in Table 5.

For the PA11/FR/K formulations, thermal stability, flammability, mechanical, and morphological microstructure analysis were performed. For the microstructure analysis, only formulation 70N_20FR_10K was analyzed.

Table 5: PA11/FR/K matrix

Formulation	*PA11 (wt.%)*	*Fire-retardant (wt.%)*	*Kraton (wt.%)*
PA11	100	-	-
80N_20FR	80	20	-
75N_20FR_5K	75	20	5
70N_20FR_10K	70	20	10
65N_20FR_15K	65	20	15
60N_20FR_20K	70	20	20

4.1.1 THERMAL STABILITY ANALYSIS

TGA was performed on neat PA11, K, and FR/K-reinforced PA11 under nitrogen using scan rates of 10ºC/min. The results from the TGA analysis indicate that all formulations with FR additives have lower onset degradation temperature as compared to both neat PA11 and K. All FR- modified formulations have slightly different degradation curves as it can be seen in Figure 4. K has higher onset degradation temperature than PA11 and all FR-modified formulations. K is more thermally stable than all formulations before 450ºC, but then starts to degrade at a faster rate.

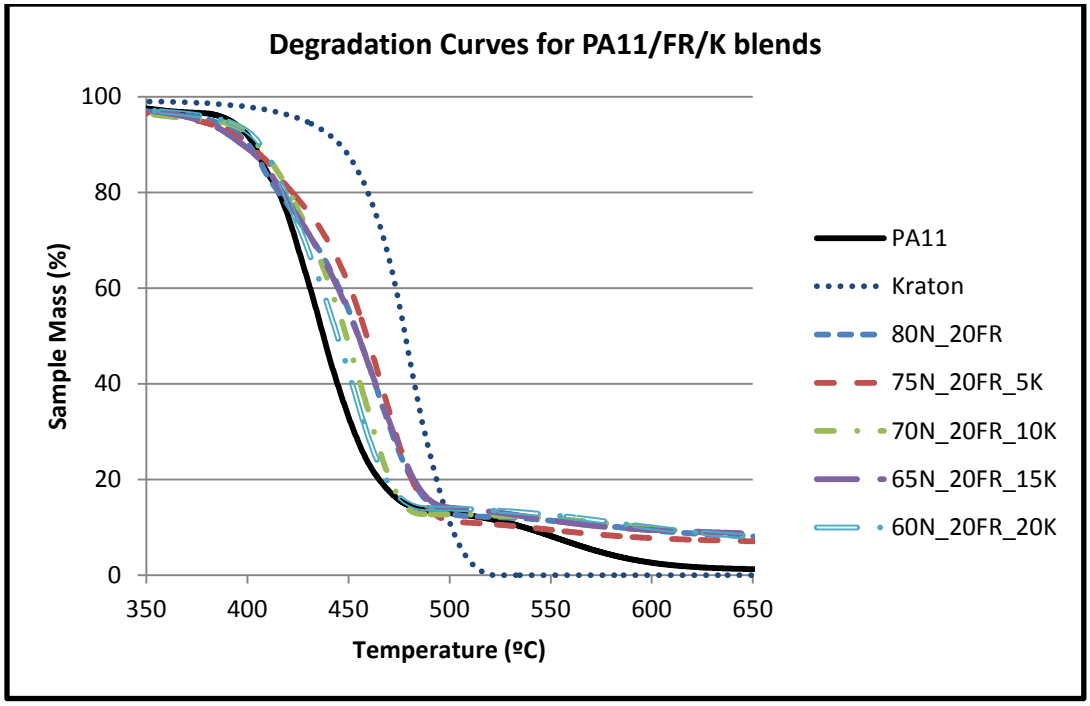

Figure 4: Degradation curves PA11/FR/K blends (TGA, scan rate 10ºC/min in N_2.

The decomposition temperatures for both 10% and 50% mass loss, $T_{10\%}$ and $T_{50\%}$, were measured and summarized in Table 1. The $T_{10\%}$ for neat PA11 and K are 403 ºC and 445ºC, respectively. PA11's $T_{10\%}$ is slightly higher than the formulations with 0%, 5%, and 15% K concentration by about 3 to 6 ºC. The formulations with 10% and 20% K concentration show a slight increase in $T_{10\%}$ of about 1 to 3°C when compared to neat PA11. K's $T_{10\%}$ is significantly higher than all other formulations. The $T_{50\%}$ for neat PA11 is 438°C, which is lower than all other formulations containing FR and K. After heating the materials to 1000°C, neat PA11 has only 0.88% of char residue left whereas the char residue for all other formulations with FR additive significantly increased to about 6-7wt%. K's $T_{50\%}$ is 478ºC, which is about 20ºC higher than all other formulations, and it

has no char residue left, which can explain why the concentration of K appears to have very little effect on the amount of char formation. Overall, K appears to have very little effect on the thermal degradation behavior of the blends.

Table 6: Decomposition temperature of PA11/FR/K blends

	$T_{10\%}$ (°C)	$T_{50\%}$ (°C)	Residue Mass at 1000°C (%)
PA11	403	438	0.88
Kraton	445	478	0
80N_20FR	400	455	7.7
75N_20FR_5K	400	459	6.5
70N_20FR_10K	405	449	7.5
65N_20FR_15K	397	455	7.7
60N_20FR_20K	406	445	7.2

4.1.2 FLAMMABILITY ANALYSIS

4.1.2.1 MCC

When compared, neat PA11 has lower heat release capacity and peak heat release rate than K as shown in both Figure 5 and Table 7. As a consequence, one would expect for K to negatively affect the flammability properties of PA11 even after it is blended with FR additives. The MCC results correlate with this assumption for all formulations containing K. The heat release capacity is higher in all the formulations with K. The formulation with 15% has the highest value and this value decreases when the concentration of K reaches 20%. Furthermore, just the addition of 20% FR brought the heat release capacity and peak heat release rate of PA11 to a low value of 577 and 673, respectively, indicating the positive effect it has decreasing the flammability of PA11.

From Figure 5, it can also be concluded that the peak heat release rate for neat PA11 occurred at a lower temperature than all other formulations, but K.

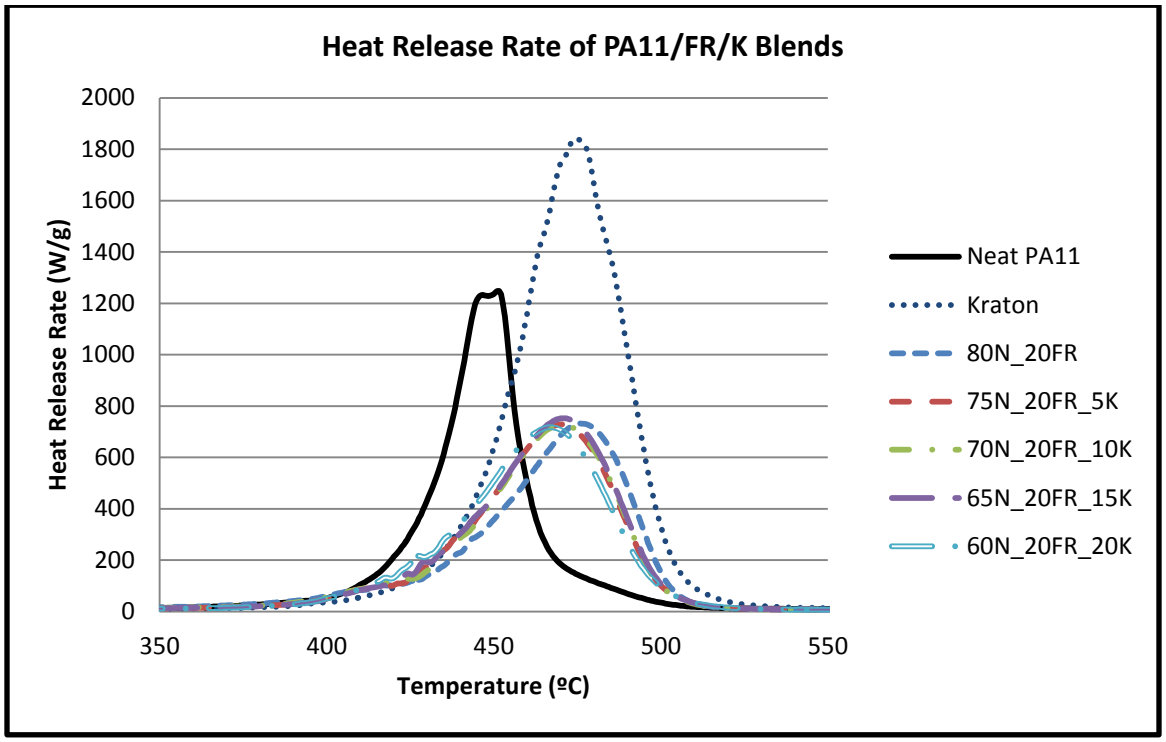

Figure 5: Heat release rate of PA11/FR/K blends.

Table 7: Summary of MCC results for PA11/FR/K blends

	Heat Release Capacity (J/g-K)	***SD***	***Peak Heat Release (W/g)***	***SD***
PA11	1113	50	1277	46
Kraton	1311	19	1786	59
80N_20FR	577	3	673	3
75N_20FR_5K	601	21	701	24
70N_20FR_10K	616	9	718	10
65N_20FR_15K	640	30	746	35
60N_20FR_20K	617	12	720	15

4.1.2.2 UL 94

A total of five samples for each formulation were tested. Figure 6: UL 94 samples. From left to right: PA11, 80N_20FR, 75N_20FR_ 5K, 70N_20FR_10K, 65N_20FR_15K, 60N_ 20FR_ 20K.

Table 8 summarizes the UL 94 test results. From the data gathered, only formulation 80N_20FR passed the V-0 rating. In addition, the results from the MCC do not correlate well with the UL 94 results since 70N_20FR_10K was almost rated V-0, and formulation 60N_20FR_20K has about the same heat release capacity and heat release rate, but it dripped and was rated V-2. Figure 6 shows the post-test UL 94 specimens.

Figure 6: UL 94 samples. From left to right: PA11, 80N_20FR, 75N_20FR_ 5K, 70N_20FR_10K, 65N_20FR_15K, 60N_ 20FR_ 20K.

Table 8: UL 94 results for PA11/FR/K blends

Formulation	*Average 1st burn flaming combustion duration (s)*	*Averaged 2nd burn flaming combustion duration (s)*	*Flaming Drip*	*UL 94 Rating*
PA11	4	-	Yes	V-2
80N_20FR	8	9	No	V-0
75N_20FR_5K	16	13	No	V-1
70N_20FR_10K	14.6	12.4	No	V-1
65N_20FR_15K	21.3	-	Yes	V-2
60N_20FR_20K	22	-	Yes	V-2

4.1.3 MECHANICAL PROPERTIES RESULTS AND DISCUSSION

Table 9 summarizes the mechanical properties of the PA11/FR/K blends, K, and ALM's material. It is known from previous studies that the addition of FR additives and nanoparticles into the polymer matrix has a deleterious effect in the elongation at break, which is typically decreased by more than 90% [7, 13, 20, 24]. The values for K shown in Table 9 were gathered from the technical data sheet provided by the manufacturer where the properties were determined on a film cast from toluene solution and were used for comparison purposes in this analysis. Similarly, the mechanical properties of ALM's material were gathered from the technical data sheet provided by the manufacturer where the properties are based on SLS parts while our data are based on injection molding. As expected from the literature, the elongation at break of PA11 was significantly reduced from 164% to about 6% by the addition of just 20% FR. K has an elongation at break of about 500% and improvements in the elongation at break of PA11 were achieved by varying the concentration of K. K at 5% slightly increased the elongation at break from 6.32% to 9.35%. The most significant result came from K at 20% with an elongation at

break of 40.1%. In contrast, as the concentration of K increased in the polymer matrix, the tensile strength of PA11 decreased from 48.5 MPa to 26.9 MPa. This value is even lower than the value of 34.5 MPa K has. ALM's material has higher tensile strength than all of our formulations and higher elongation at break than all our formulations except 60N-20FR_20K. A more appropriate comparison between ALM's and our formulations can be made if SLS specimens are made from these formulations.

Table 9: Summary of tension test results for PA11/FR/K blends

Formulation	***Tensile Strength (MPa)***	***SD***	***Modulus (MPa)***	***SD***	***Elongation at Break (%)***	***SD***
PA11	48.5	3.2	1,380	40.7	164	73.5
Kraton	34.5	-	-	-	500	-
80N_20FR	41.6	1.8	1,870	135	6.32	2.3
75N_20FR_5K	37.9	0.9	1,630	54.3	9.35	1.9
70N_20FR_10K	33.8	1.1	1,370	66.5	17.3	2.5
65N_20FR_15K	29.9	0.6	1,330	47.2	24.9	2.9
60N_20FR_20K	26.9	0.4	1,140	31.4	40.1	10.8
ALM	46	-	1,345	-	38	-

4.1.4 MORPHOLOGICAL MICROSTRUCTURAL ANALYSIS

After completion of both the UL 94 and tension tests, cross-section SEM images of formulation 70N_20FR_10K were taken. The samples were coated prior to SEM analysis since the polymer material is insulating. Representative images for both post UL 94 and tension are shown below, Figure 7 Figure 8, respectively. Figure 7 shows the formation of a hard char of FR that acts as a heat shield to protect the polymer matrix from further combustion. The FR's resistance to combustion to prevent both the PA11

and K to burn causes it to expand and create bubbles in the material. Although the FR's inherent mechanism to resist combustion, formulation 70N_20FR_10K did not achieve a V-0 rating. Figure 8 shows the fractural surface of formulation 70N_20FR_10K. From the SEM, FR additives can be seen embedded in the polymer matrix acting as defects or weak points. These defects create voids, which can help to explain the drop in strength and elongation at break. From the SEM, we were unable to analyze the microstructural mechanisms of K.

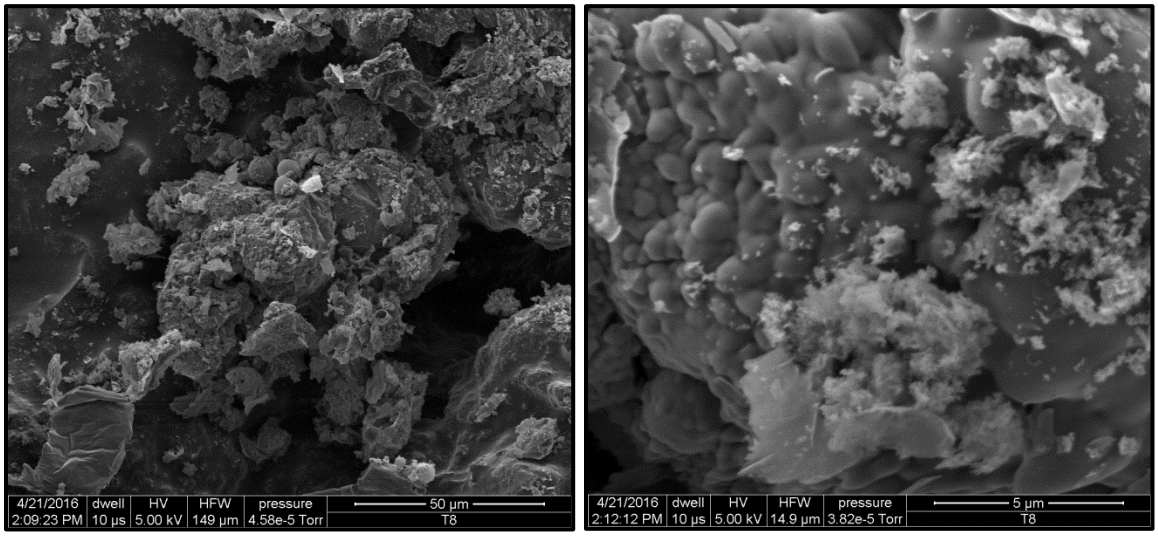

Figure 7: Post UL 94 testing SEM images of formulation 70N_20FR_10K.

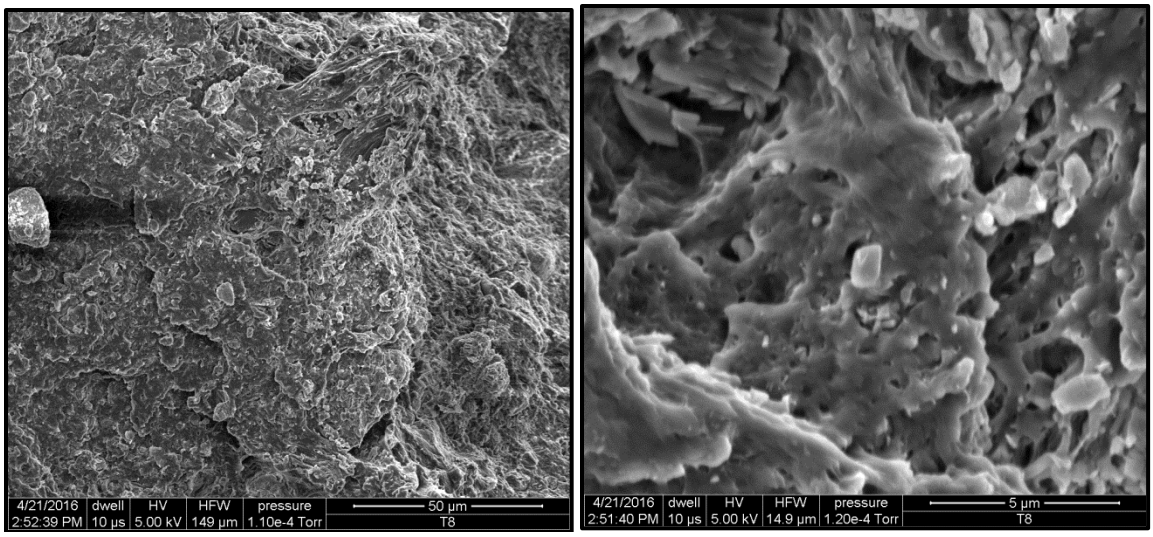

Figure 8: Post tension testing SEM images of formulation 70N_20FR_10K.

4.1.5 SUMMARY

For the first masterbatch, a feasibility study was performed to explore and analyze the effect K has on the PA11 matrix. Thermal, flammability, mechanical properties, and morphological microstructural analysis were performed. Based on this set of results, K has very little effect on the peak heat release rate and heat release capacity of PA11. The formulation with 20% FR and 10% K appears to be the best in terms of flammability and mechanical properties with an elongation at break of 17% and a V-1 UL 94 rating. The addition of 20% K brought back the elongation at break to 40%, but this formulation performed poorly in the UL 94 flammability test. Figure 8 shows the effect the concentration of K had on both the elongation at break and heat release capacity for this formulation. TGA analysis shows that the concentration of K has a slight effect on the amount of char formation and on the thermal degradation of the blends.

4.2 Results and Discussion for Second Masterbatch

Given the results from our first study and previous studies by Lao et al. suggest that a synergism effect to improve the flammability properties can be achieved by using a concentration of 5 – 7.5% of NC and 15 – 20% of FR [19, 21, 22, 25], for our second study a total of six formulations were melt-blended with a constant concentration of 10% K and different loadings of NC, and FR as shown in Table 10. It was of interest to see if a synergism effect could be achieved between the FR, K, and NC.

Same as with our first study, for the PA11/FR/K/NC formulations, thermal stability, flammability, mechanical, and morphological microstructure analysis were performed. For the microstructure analysis, only formulation 70N_20FR_10K was analyzed.

Table 10: PA11/FR/K/NC matrix

Formulation	***PA11 (wt.%)***	***Fire-Retardant (wt.%)***	***Kraton (wt.%)***	***Nanoclay (wt.%)***
70N_15FR_10K_5NC	70	15	10	5
67.5N_17.5FR_10K_5NC	67.5	17.5	10	5
65N_20FR_10K_5NC	65	20	10	5
67.5N_15FR_10K_7.5NC	67.5	15	10	7.5
65N_17.5FR_10K_7.5NC	65	17.5	10	7.5
62.5N_20FR_10K_7.5NC	62.5	20	10	7.5

4.2.1 THERMAL STABILITY ANALYSIS

TGA was performed on neat PA11 and FR/K/NC-reinforced PA11 under nitrogen using scan rates of 10°C/min. The data gathered for formulation PA11 and 70N_20FR_10K from our previous study are plotted against our new results for comparison since PA11 is our control and a 10% concentration of K was kept constant in all of the formulations. The results from the TGA analysis indicate that all formulations with FR additives and NC have lower onset degradation temperature than PA11 and about the same as formulation 70N_20FR_10K. All FR/K/NC-reinforced PA11 formulations have almost identical degradation curves as shown in Figure 9. The decomposition temperatures for both 10% and 50% mass loss, $T_{10\%}$ and $T_{50\%}$, were inferred and summarized in Table 11: Decomposition temperature of PA11/FR/K/NC blendsTable 11. All FR/K/NC-reinforced PA11 formulations are more thermally stable than PA11 and formulation 70N_20FR_K.

The $T_{10\%}$ for neat PA11 and formulation 70N_20FR_10K is 403°C and 405°C, respectively, which are higher than the rest of the formulations except for 67.5N_17.5FR_10K_5NC. Formulation 65N_20F_10E_5C has the lowest $T_{10\%}$ at 383°C. The $T_{50\%}$ for neat PA11 is 438°C, which is lower than all other formulations. Similarly, $T_{50\%}$ for 70N_20FR_10K, although higher than neat PA11, is lower than all FR/K/NC-reinforced PA11 formulations by about 20°C. After heating the materials to 1,000°C, neat PA11 has only 0.88% of char residue left whereas the char residue for all other formulations significantly increased. The NC did have an effect in char residue. The formulation without NC had a char residue of 7.5% whereas the ones with NC had an

increase in char residue ranging from 9.5% to 15.3%. The concentration of NC and FR also increases the char residue of the material. Formulations with higher concentrations of FR, NC, or both had higher char residue. Formulation 62.5N_20FR_10K_7.5NC has the highest char residue.

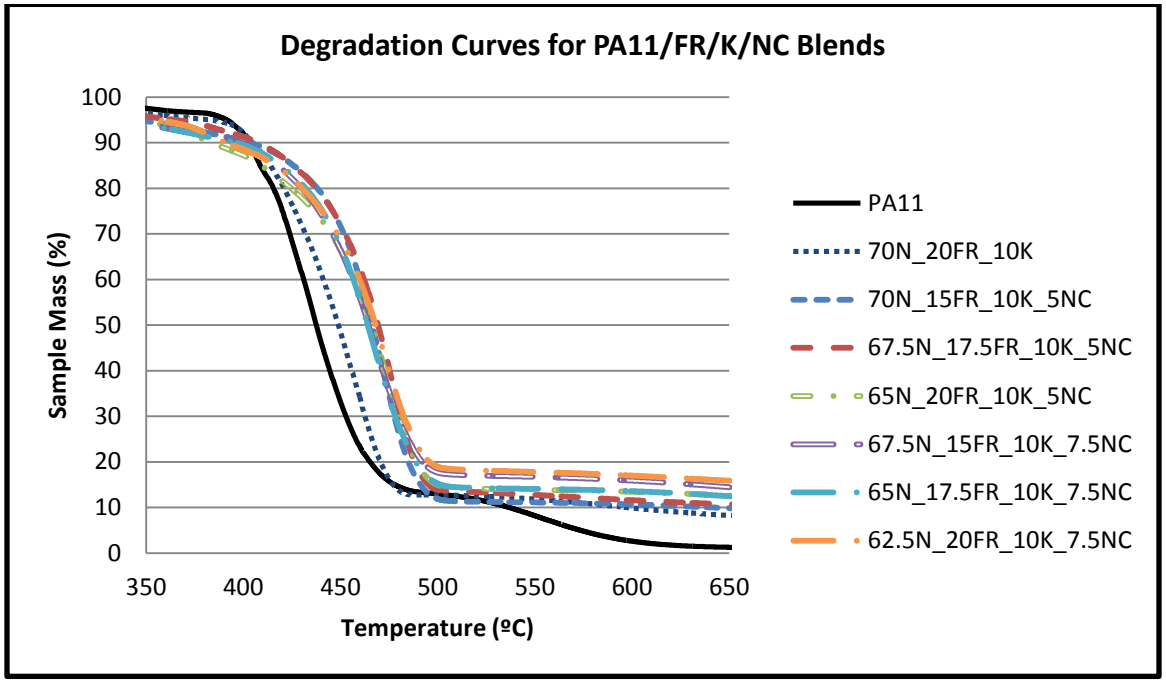

Figure 9: Degradation curves for PA11/FR/K/NC blends (TGA, scan rate 10ºC/min in N_2.

Table 11: Decomposition temperature of PA11/FR/K/NC blends

	$T_{10\%}$ (°C)	$T_{50\%}$ (°C)	Residue Mass at 1000°C (%)
PA11	403	438	0.88
70N_20FR_10K	405	448	7.5
70N_15FR_10K_5NC	403	466	9.5
67.5N_17.5FR_10K_5NC	407	469	10.6
65N_20FR_10K_5NC	383	466	12.2
67.5N_15FR_10K_7.5NC	399	465	12.8
65N_17.5FR_10K_7.5NC	396	463	10.8
62.5N_20FR_10K_7.5NC	391	468	15.3

4.2.2 FLAMMABILITY ANALYSIS

4.2.2.1 MCC

Applied Laser Materials (ALM) has a commercially available fire-retardant PA11 powder for SLS. This material was compared to our FR/K and FR/K/NC-reinforced PA11 formulations. Figure 10 shows that ALM's formulation reaches its peak heat release rate at a lower temperature than any of our formulations. One more thing to notice is the shape of ALM's curve. The heat release rate appears to increase at a higher rate at the beginning and then the heat release rate seems to increase at a decreasing rate to then continue to increase at a higher rate again. This is still under investigation.

The addition of NC seems to bring down slightly the peak heat release rate and heat release capacity of the formulations when compared to formulation 70N_20FR_10K from our previous study. Table 12 summarizes all these results. The ALM's formulation has a heat release rate of about 540 J/g-K and a peak heat release rate of about 605 W/g, which is relatively better than most of our formulations except 62.5N_20F_10K_7.5NC. It is also noticed the peak heat release rate temperature of the ALM material occurs at 440^{o}C while our formulations occur at 480^{o}C (Figure 10). The higher concentration of FR, NC, or both seems to yield a lower peak heat release rate and heat release capacity.

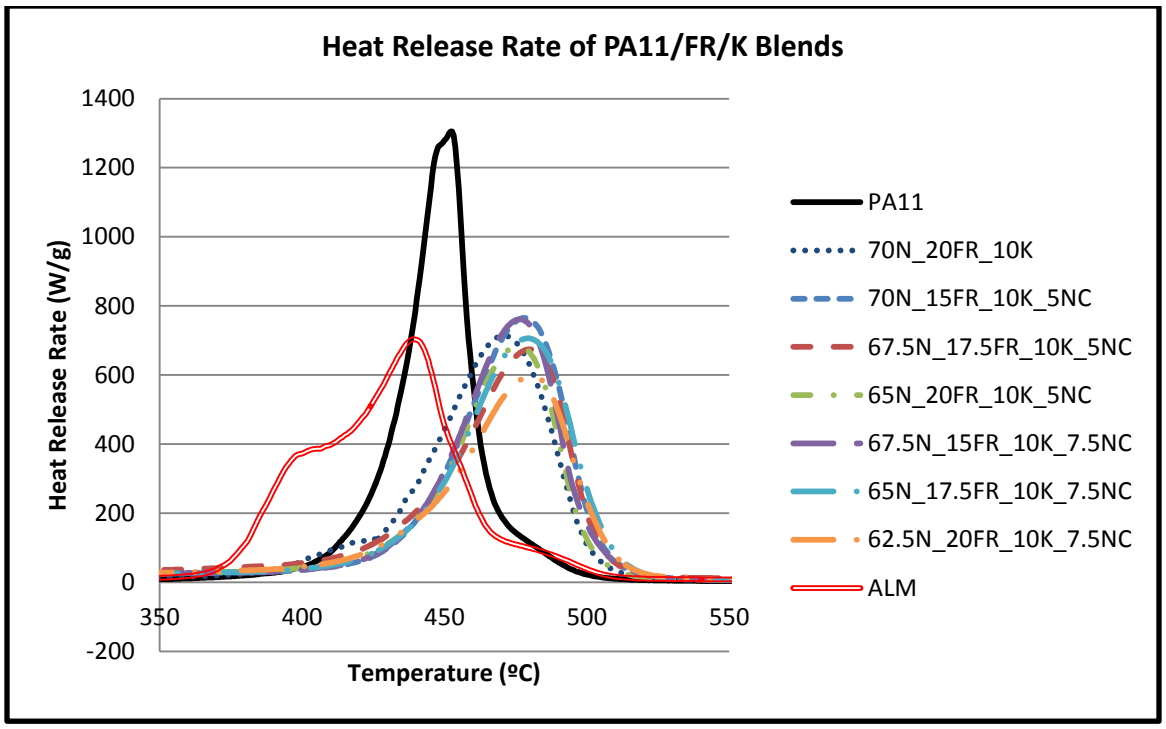

Figure 10: Heat release rate of PA11/FR/K/NC blends.

Table 12: Summary of MCC results for PA11/FR/K/NC blends

	Heat Release Capacity (J/g-K)	***SD***	***Peak Heat Release (W/g)***	***SD***
PA11	1112	50	1277	46
70N_20FR_10K	616	9	718	10
70N_15FR_10K_5NC	648	6	756	8
67.5N_17.5FR_10K_5NC	581	41	679	47
65N_20FR_10K_5NC	605	32	640	39
67.5N_15FR_10K_7.5NC	599	10	699	11
65N_17.5FR_10K_7.5NC	604	18	705	21
62.5N_20FR_10K_7.5NC	563	27	605	28
ALM	540	27	605	28

4.2.2.2 UL 94

A total of five samples for each formulation were tested. Table 13 summarizes the UL 94 test results of the formulations. From the data gathered, none of the formulations passed the V-0 requirement. In addition, the results from the MCC do not correlate well with the UL 94 results, since 70N_20FR_10K was almost rated V-0 and had significantly higher heat release capacity than most of the formulations with NC. One thing to notice is that all formulations for the exception of 62.5N_20FR_10K_7.5NC seem to have a longer first burn flaming combustion duration. Another thing to notice is that none of the formulations except for neat PA11 dripped and burned the cotton placed at the bottom of the samples. When the samples were burned, it was also noticed that only a very small portion of the sample remained burning before self-extinguishing, which gave higher times and a V-1 rating. This raises the questions of how well dispersed were both the FR additive and NC in the polymer matrix. Figure 11 shows the samples after the UL 94 test was conducted, which visually correlates with the time it took each sample to self-extinguish. From all these formulations, it can be conclude from both the time it took each formulation to self-extinguish and Figure 11 that formulation 70N_20FR_10K is the best in this test.

Table 13: UL 94 results for PA11/FR/K/NC blends

Formulation	Average 1st burn flaming combustion duration (s)	Averaged 2nd burn flaming combustion duration (s)	Flaming Drip	UL 94 Rating
PA11	4	-	Yes	V-2
70N_20FR_10K	14.6	12.4	No	V-1
70N_15FR_10K_5NC	30	10	No	V-1
67.5N_17.5FR_10K_5NC	23.6	6.6	No	V-1
65N_20FR_10K_5NC	15.6	7.4	No	V-1
67.5N_15FR_10K_7.5NC	30	11	No	V-1
65N_17.5FR_10K_7.5NC	18.5	6.4	No	V-1
62.5N_20FR_10K_7.5NC	13	18	No	V-1

Figure 11: UL 94 samples. From left to right: PA11, 70N_20FR_10K, 70N_15FR_ 10K _ 5NC, 67.5N_17.5FR_10K_5NC, 67.5N_15FR_10K_ 7.5NC, 65N_ 20FR_ 10K_5NC, 65N_17.5FR_10K_7.5NC, and 62.5N_20FR_10K_7.5NC.

4.2.3 MECHANICAL PROPERTIES

Table 14 summarizes the room temperature mechanical properties of blends containing FR, K, and NC. From our previous study, it was shown that 20% FR brings the elongation at break down to 6%. The addition of 10% K brought the elongation back to 17%. It was of interest to see how the elongation at break would be affected by the NC since it is also known that NC has a negative effect on elongation at break. The addition of NC improved the modulus by almost 50% with 62.5N_20FR_10K_7.5NC having the highest modulus. The tensile strength does not change with different concentrations of FR and NC, but it is lower than neat PA11. Elongation at break was drastically affected by the addition of NC. The higher the concentration of NC the lower the elongation at break with reading as low as 3%, which is even lower than the 6% obtained in our previous study. ALM's material has higher tensile strength and elongation at break than all of our formulations. A more appropriate comparison between ALM's and our formulations can be made if SLS specimens are made with these formulations.

Table 14: Summary of tension test results for PA11/FR/K/NC blends

Formulation	*Tensile Strength (MPa)*	*SD*	*Modulus (MPa)*	*SD*	*Elongation at Break (%)*	*SD*
PA11	49	3	1,380	41	164	74.5
70N_20FR_10K	34	1	1,320	67	17	2.5
70N_15FR_10K_5NC	36	2	1,920	47	8	0.7
67.5N_17.5FR_10K_5NC	35	1	2,050	67	8	0.6
65N_20FR_10K_5NC	34	1	2,060	142	7	1.2
67.5N_15FR_10K_7.5NC	37	2	2,310	44	3	0.1
65N_17.5FR_10K_7.5NC	34	5	2,310	106	3	0.9
62.5N_20FR_10K_7.5NC	34	2	2,460	132	3	0.1
ALM	46	-	1,345	-	38	-

4.2.4 MORPHOLOGICAL MICROSTRUCTURAL ANALYSIS

After completion of both the UL 94 and tension tests, the formulation with the overall best mechanical and flammability properties was chosen and cross-section SEM images were taken. Formulation 67.5N_17.5FR_10K_5NC was chosen. The samples were coated prior to SEM analysis since the polymer material is insulating. Representative images for both post UL 94 and tension are shown below in Figure 12Figure 13, respectively. Figure 12 shows the post UL 94 testing SEM images. As the specimen was ignited, the FR acted as a heat shield to protect the polymer matrix by expanding and resisting combustion. From the SEM, it can be seen that a large amount of bubbles were created in the attempt of the FR's inherent mechanism to resist combustion. This formulation, however, did not achieve a V-0 rating. The fractural surface of formulation 67.5N_17.5FR_10K_5NC can be seen in Figure 13. A large amount of voids can be seen throughout the cross section of the specimen, which can help to explain the drop in strength and elongation at break.

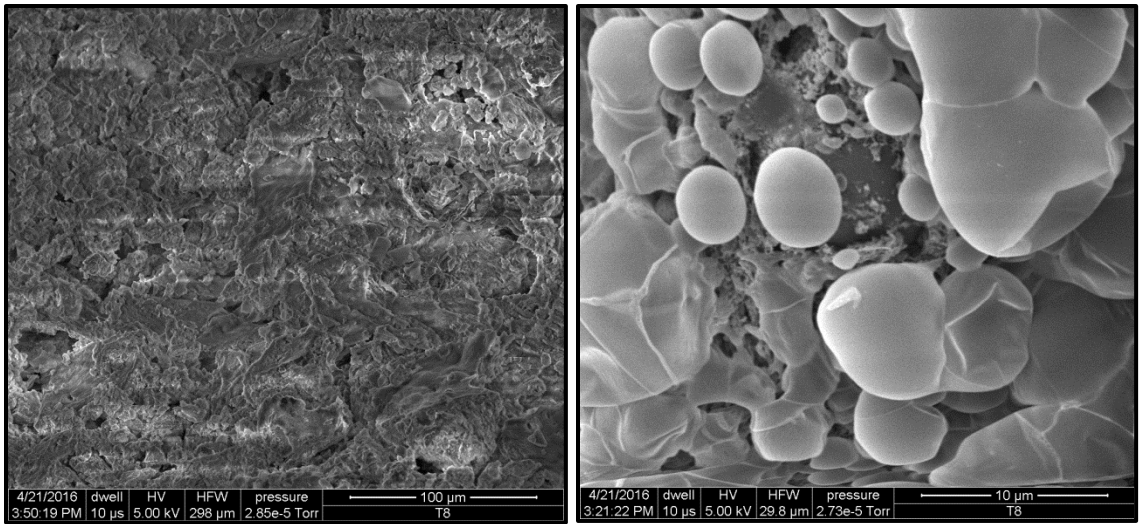

Figure 12: Post UL 94 testing SEM images of formulation 67.5N_17.5FR_10K_5NC.

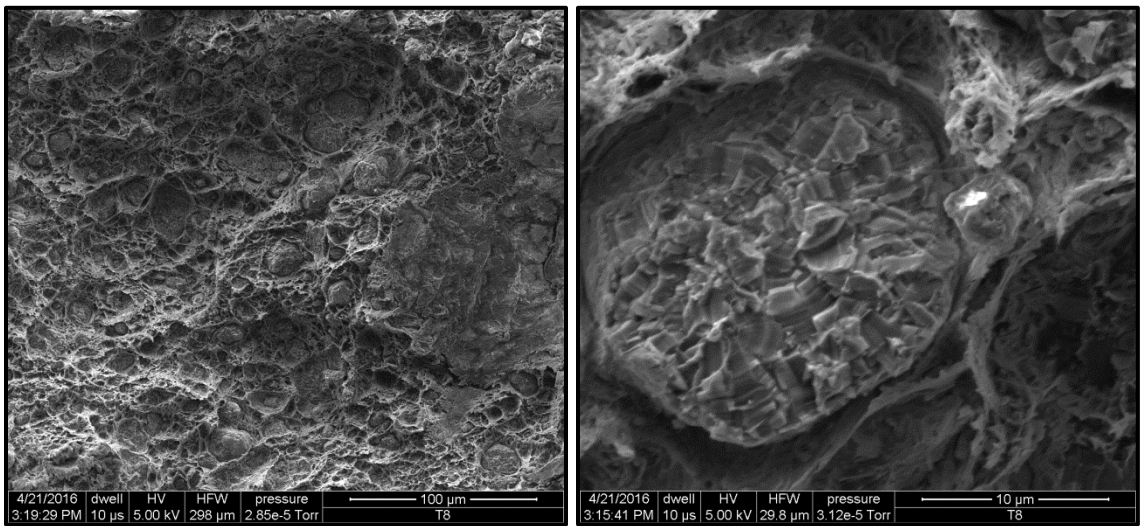

Figure 13: Post tension testing SEM images of formulation 67.5N_17.5FR_10K_5NC.

4.2.5 SUMMARY

For the second masterbatch, a feasibility study was performed to explore the potential of using a FR additive, K, and NC to improve the flammability properties of PA11 from our previous study while maintaining the mechanical properties achieved by adding 10% K. Thermal, flammability, mechanical properties, and morphological

microstructural analysis were performed. These formulations did not reach the desired mechanical and flammability properties via injection molding; hence, making specimens via SLS is not economically feasible yet. Based on this set of results, the addition of NC and the FR additive gives a higher char residue when compared to neat PA11. In addition, NC brought the peak heat release and heat release capacity lower and close to the commercially available ALM's PA11 powder with 62.5N_20F_10E_7.5C being the best formulation in this set of experiments. Unfortunately, none of the formulations achieved a V-0 rating even though the MCC results seemed promising when compared to the ALM formulation. Additionally, the elongation at break property for all the formulations with NC performed poorly.

4.3 RESULTS AND DISCUSSION FOR THIRD MASTERBATCH

The results from our second study were not encouraging. There was not a synergism effect between the FR, K, and NC. Hence for our third and final study, we studied the combined effects of FR, K, NC, and MWNTs on the mechanical and flammability properties. Our final study is based on the study carried out by Johnson et al. [20] in which they successfully achieved a V-0 rating. They were able to achieve this by using 15% FR and the addition of two nanoparticles, NC and CNFs, at either 2.5% or 3.5% wt. loading each. Although they were able to meet the V-0 rating, the elongation at break still suffered with a low value of about 4%. It is of interest to see the effect K will have on this PA11 matrix. For our study, we replaced CNFs by MWNTs. Table 15 shows the matrix used for this study.

Same as with our two previous studies, for the PA11/FR/K/NC/MWNT formulations, thermal stability, flammability, mechanical, and morphological microstructure analysis were performed. Since the amount of material that needs to be compounded to make tension and UL 94 specimens for all six formulations is quite a large experiments to be conducted, and it requires a lot of time, it was decided that only enough material to do UL 94 testing for each formulation and two formulations for tension testing would be made. For the tension test, the two formulations were chosen based on the MCC results. For the microstructural analysis, only one formulation was analyzed.

Table 15: PA11/FR/K/NC/MWNT matrix

Formulation	*PA11 (wt.%)*	*Fire-Retardant (wt.%)*	*Kraton (wt.%)*	*Nanoclay (wt.%)*	*MWNTs (wt.%)*
1	70	15	10	2.5	2.5
2	65	15	15	2.5	2.5
3	60	15	20	2.5	2.5
4	68	15	10	3.5	3.5
5	63	15	15	3.5	3.5
6	58	15	20	3.5	3.5

4.3.1 THERMAL STABILITY ANALYSIS

TGA was performed on FR/K/NC/MWNT-reinforced PA11 under nitrogen using scan rates of 10°C/min as shown in Figure 14. The results from the TGA analysis indicate that all FR/K/NC/MWNT-PA11 reinforced formulations have slightly lower

onset degradation temperature than PA11. All FR/K/NC/MWNT-PA11 reinforced formulations for the exception of 65N_15FR_15K_2.5NC_2.5MWNT have identical degradation curves as shown in Figure 14. The decomposition temperatures for both 10% and 50% mass loss, $T_{10\%}$ and $T_{50\%}$, were measured and summarized in Table 16. All FR/K/NC/MWNT-PA11 formulations are more thermally stable than PA11.

There is no apparent trend in the $T_{10\%}$ for any of the formulations. At $T_{10\%}$, PA11 is at 403°C and only formulations 65N_15FR_15K_2.5NC_2.5MWNT and 58N_15FR_20K_3.5NC_3.5MWNT have higher $T_{10\%}$ at 410°C and 411°C, respectively. The $T_{50\%}$ for all FR/K/NC/MWNT-PA11 reinforced formulations is about the same at 468°C for the exception of formulation 65N_15FR_15FR_2.5_2.5, which is higher at 485°C. After heating the materials to 1,000°C, neat PA11 has only 0.88% of char residue left whereas the char residue for all other formulations significantly increased to a low of 6.68% to a high of 11.3%. There is no apparent trend in the effect higher concentrations of NC, MWNT, or K have on the char residue.

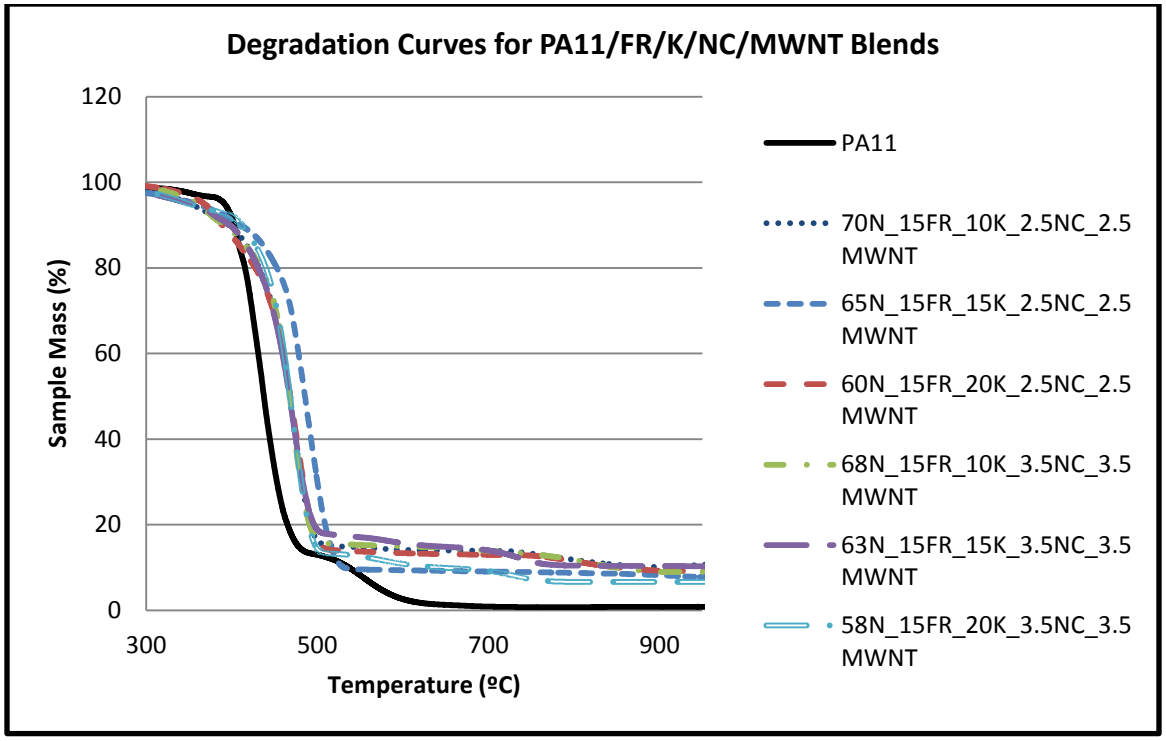

Figure 14: Degradation curves PA11/FR/K/NC/MWNT blends (TGA, scan rate 10ºC/min in N_2.

Table 16: Decomposition temperature of PA11/FR/K/NC/MWNT blends

	$T_{10\%}$ (°C)	$T_{50\%}$ (°C)	Residue Mass at 1000°C (%)
PA11	403	438	0.88
70N_15FR_10K_2.5NC_2.5MWNT	396	467	11.3
65N_15FR_15K_2.5NC_2.5MWNT	410	485	7.39
60N_15FR_20K_2.5NC_2.5MWNT	389	468	9.21
68N_15FR_10K_3.5NC_3.5MWNT	391	468	8.98
63N_15FR_15K_3.5NC_3.5MWNT	397	467	10.13
58N_15FR_20K_3.5NC_3.5MWNT	411	468	6.68

4.3.2 FLAMMABILITY ANALYSIS

4.3.2.1 MCC

Similarly to our last masterbatch, we compared our formulations to ALM's commercially available FR PA11 powder for SLS. Figure 15 shows that ALM's formulation reaches its peak heat release rate at a lower temperature than any of our formulations including PA11. Both the heat release capacity and peak heat release rate of ALM are lower than all of our formulations. With formulations 60N_15FR_20K_2.5NC_2.5MWNT and 60N_15FR_15K_2.5NC_2.5MWNT having the lowest heat release capacity and peak heat release rate, respectively, of our formulations. Overall, the formulations with 3.5% NC and MWNT appear to a lower heat release capacity, but higher peak heat release rate. Table 17 summarizes all these results.

Table 17: Summary of MCC results for PA11/FR/K/NC/MWNT blends

Formulation	***Heat Release Capacity (J/g-K)***	***SD***	***Peak Heat Release Rate (W/g)***	***SD***
PA11	1112	50	1277	46
70N_15FR_10K_2.5NC_2.5MWNT	648	11	896	20
65N_15FR_15K_2.5NC_2.5MWNT	688	15	758	19
60N_15FR_20K_2.5NC_2.5MWNT	576	16	795	20
68N_15FR_10K_3.5NC_3.5MWNT	625	36	863	48
63N_15FR_15K_3.5NC_3.5MWNT	619	46	856	65
58N_15FR_20K_3.5NC_3.5MWNT	632	30	866	39
ALM	540	27	605	28

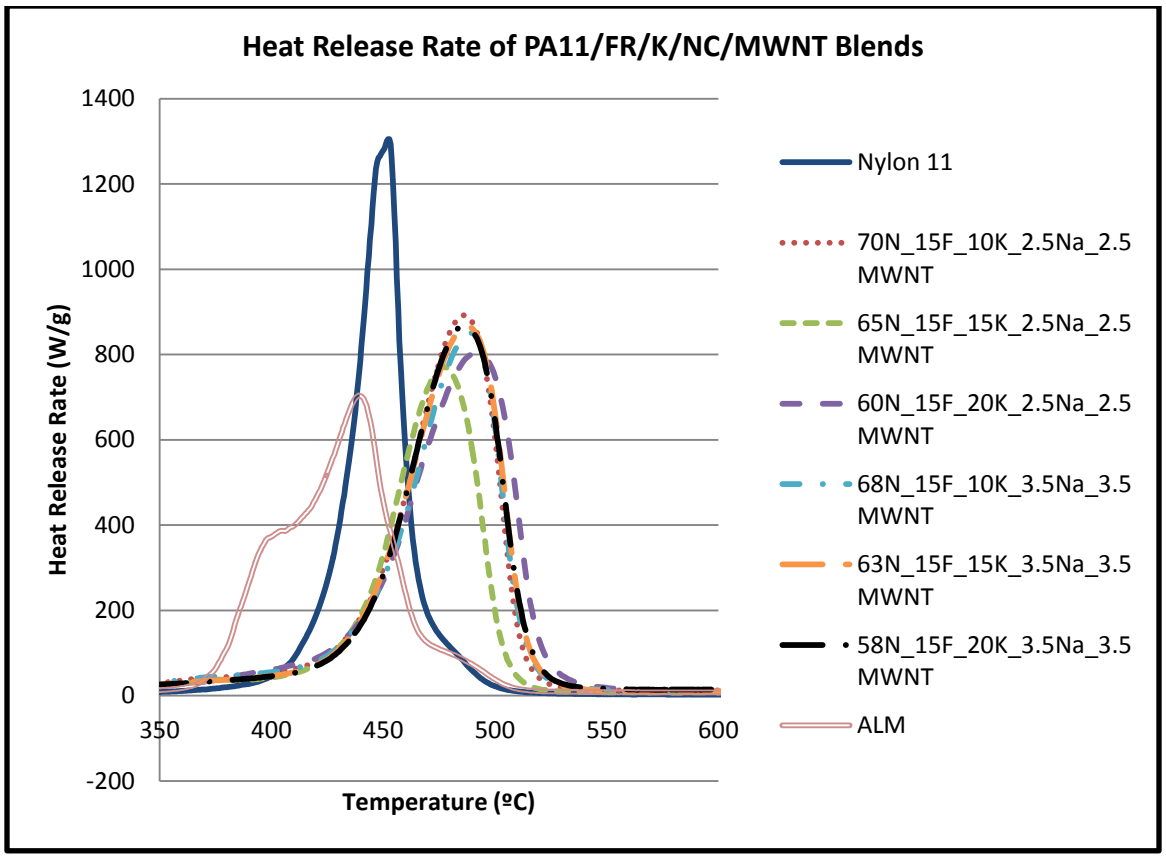

Figure 15: Heat release rate of PA11/FR/K/NC/MWNT blends.

4.3.2.2 UL 94

A total of five samples for each formulation were tested. Table 18 summarizes the UL 94 test results of the formulations. From the data gathered, the results are quite promising. Similar results were found as the ones found our last batch is focused on [20]. All of the formulations passed the V-0 requirement. They all did not drip and immediately self-extinguished. Figure 16 shows the tested samples and how they are barely show any signs of being burned after the test. There was not a difference between the K, NC, and MWNT concentrations and the time each formulation took to self-

extinguish. From these results, it can be concluded that there is a synergistic effect between FR, NC, and MWNT in improving the flammability of PA11.

Table 18: UL 94 results for PA11/FR/K/NC/MWNT blends

Formulation	***Average 1st burn flaming combustion duration (s)***	***Averaged 2nd burn flaming combustion duration (s)***	***Flaming Drip***	***UL 94 Rating***
70N_15FR_10K_2.5MWNT_2.5Na	2	3	No	V-0
60N_15FR_20K_2.5MWNT_2.5Na	3	1	No	V-0
65N_15FR_15K_2.5MWNT_2.5Na	2	2	No	V-0
68N_15FR_10K_3.5MWNT_3.5Na	3	1	No	V-0
63N_15FR_15K_3.5MWNT_3.5Na	2	1	No	V-0
58N_15FR_20K_3.5MWNT_3.5Na	2	2	No	V-0

Figure 16: UL 94 samples. From left to right: 70N_15FR_10K_2.5NC_2.5MWNT, 65N_15FR_ 15K _ 2.5NC_2.5MWNT, 60N_15FR_20K_2.5NC_2.5MWNT, 68N_15FR_10K_ 3.5NC_3.5MWNT, 63N_ 15FR_ 15K_3.5NC_3.5MWNT, and 58N_15FR_20K_3.5NC_3.5MWNT.

4.3.3 MECHANICAL PROPERTIES

For this batch, only two formulations were tension tested, 60N_15FR_20K_2.5NC_2.5MWNT and 63N_15FR_15K_3.5NC_3.5MWNT. We chose these formulations based on the MCC results. These two formulations had the lowest heat release capacity out of all the formulations in the third batch. Table 19 summarizes the room temperature mechanical properties of the blends. It is known from our previous studies that the main impact of the FR and NC on mechanical properties lies in the elongation at break, which is typically decreased by more than 90%. It was also shown in our first study that the addition of 10% K brings the elongation back to 17%. For our second study, NC had a negative impact in the elongation at break by bringing it lower than on our first study. It was of interest to see how the elongation at break would be affected by the combined effects of FR, K, NC, and MWNT.

There was a decrease in the tensile strength for the two formulations tested. PA11 has a tensile strength of 49 MPa and both formulations have a tensile strength of 33 MPa. This is a similar trend observed in our previous studies where the tensile strength decreased by the addition of the FR, K, and a nanoparticle. The addition of both NC and MWNTs, however, did increase the modulus for both formulations. Although the elongation at break decreased from 164% to 17 and 30%, these values are higher than the 4% Johnson et al. reported in their paper with a similar formulation to ours, but without the addition of K [20]. Also, the highest elongation at break value reported by us in both of our previous studies is 40%, and this formulation dripped and failed the UL 94 test with a V-2 rating. ALM's material has higher tensile strength and elongation at break

than all of our formulations, but lower modulus. A more appropriate comparison between ALM's and our formulations can be made after SLS specimens are made.

Table 19: Summary of tension test results for PA11/FR/K/NC/MWNT blends

Formulation	*Tensile Strength (MPa)*	*SD*	*Modulus (MPa)*	*SD*	*Elongation at Break (%)*	*SD*
PA11	49	3	1,380	41	164	74
60N_15FR_20K_2.5NC_2.5MWNT	33	1.2	1,460	33.5	30	1.7
63N_15FR_15K_3.5NC_3.5MWNT	33	0.9	1,716	18.2	17	3.3
ALM	46	-	1,345	-	38	-

4.3.4 MORPHOLOGICAL MICROSTRUCTURAL ANALYSIS

After completion of both the UL 94 and tension tests, the formulation with the overall best mechanical and flammability properties was chosen and cross-section SEM images were taken. Formulation 60N_15FR_20K_2.5NC_2.5MWNT was chosen. The samples were coated prior to SEM analysis. Representative images for both post UL 94 and tension are shown below in Figure 17 Figure 18 , respectively. Figure 17 shows the post UL 94 testing SEM images. Similar to our previous studies, the FR acted as a heat shield to protect the polymer matrix by expanding and resisting combustion. From the SEM, it can be seen that in comparison to our previous studies not that many bubbles were created in the attempt of the FR's inherent mechanism to resist combustion. This could be attributed to the synergism between the FR, NC, and MWNT. The fractural surface of formulation 60N_15FR_20K_2.5NC_2.5MWNT can be seen in Figure 18. A large amount of voids can be seen throughout the cross section of the specimen, which can help to explain the drop in strength and elongation at break.

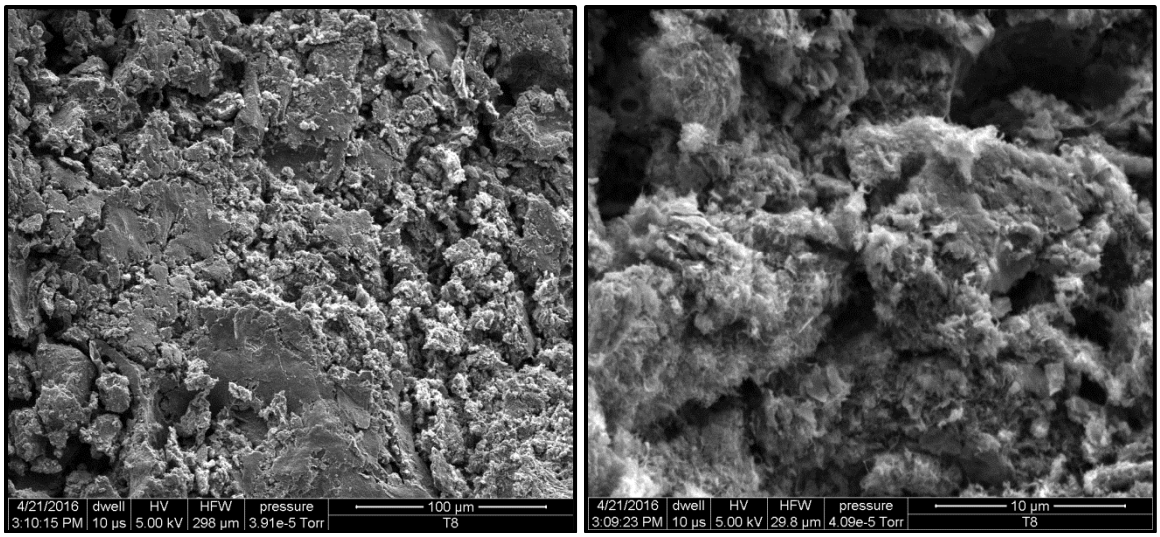

Figure 17: Post UL 94 testing SEM images of formulation 60N_15FR_20K_2.5NC_2.5MWNT.

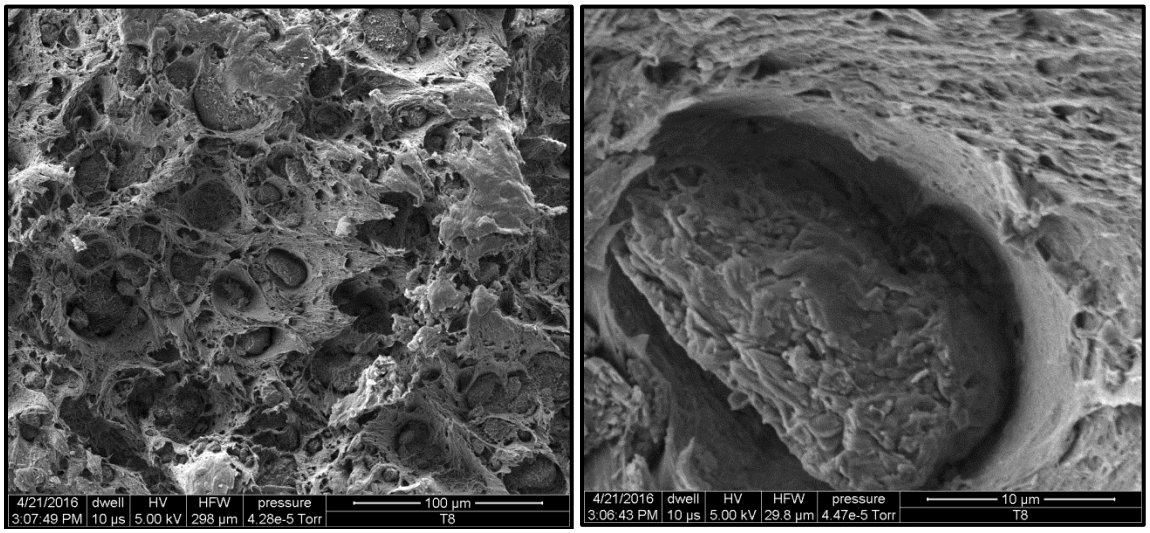

Figure 18: Post tension testing SEM images of formulation 60N_15FR_20K_2.5NC_2.5MWNT.

4.3.5 SUMMARY

For our last masterbatch, a feasibility study was performed to explore and analyze the combined effect of FR, K, NC, and MWNT in the PA11 matrix. Thermal, flammability, mechanical properties, and morphological microstructural analysis were performed. Based on this set of results, there is a synergism effect between these components. A UL 94 V-0 rating was achieved for all formulations and overall better elongation at break than our previous studies.

CHAPTER 5: CONCLUSION AND FUTURE WORK

5.1 Conclusion

Three feasibility studies were performed to explore the potential of using SLS as a fabrication method for polymer nanocomposites made using a FR additive, an elastomer, NC, and MWNT. Thermal, flammability, and mechanical properties of FR/K/NC/MWNT-reinforced PA11 nanocomposites were compared by first preparing the formulations via twin screw melt mixing method, and then, injection molding specimens. It's important to notice that SLS specimens have not yet been made using any of the formulations discussed in this thesis.

Based on these results, formulation 60N_15FR_20K_2.5NC_2.5MWNT appears to be the best in regards to flammability and mechanical properties with an elongation at break of 30% and a V-0 rating. Figure 19 shows an elongation at break and heat release capacity comparison between the best formulations in each of our studies, and it supports our conclusion about formulation 60N_15FR_20K_2.5NC_2.5MWNT. Out of the formulations tested during these studies, only the formulation 80N_20FR and the formulations with FR/K/NC/MWNT achieved a UL 94 V-0 rating. The two formulations with FR/K/NC/MWNT that were subjected to tension tests showed better elongation at break properties than all other reinforced formulations for the exception of 60N_20FR_20K. Due to time constraints, the other four FR/K/NC/MWNT formulations were not subjected to tension tests, but given the trends found in these studies, one can speculate that 60N_15FR_20K_2.5NC_2.5MWNT would still have the highest

elongation at break value since it has the lowest concentration of both NC and MWNT and the highest concentration of K.

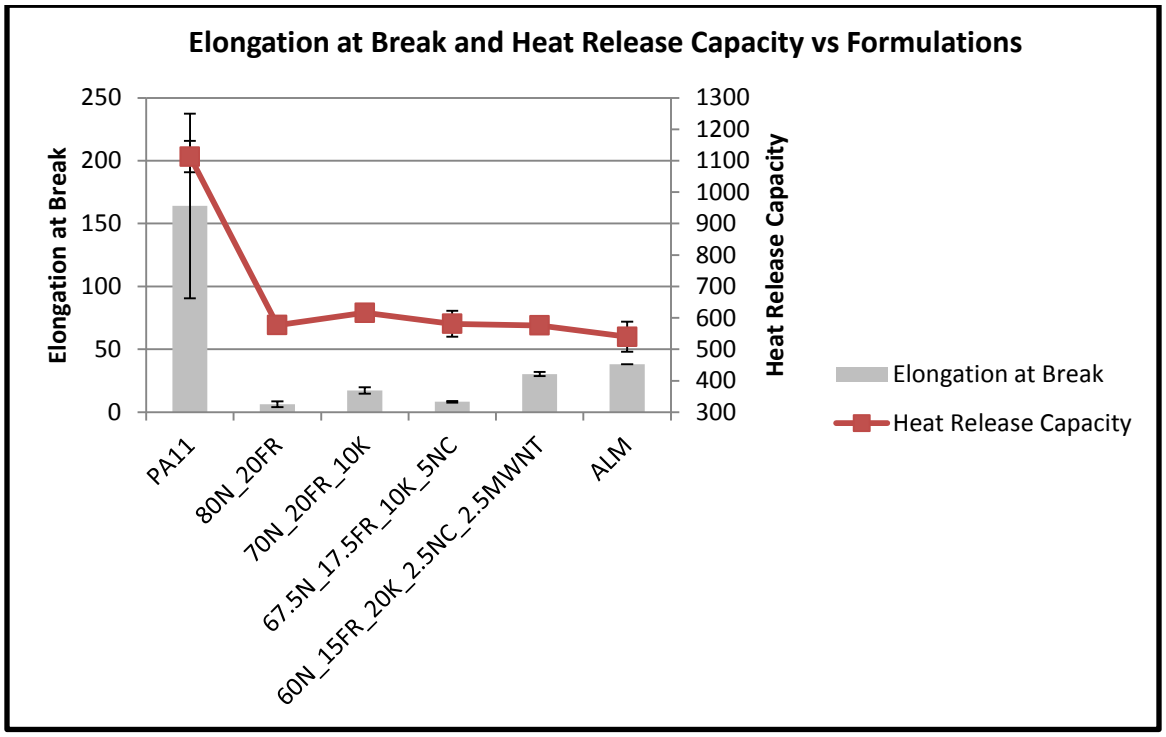

Figure 19: Elongation at break and heat release capacity comparison between multiple formulations.

Although still at its early years, SLS continues to fascinate researchers from both the academia and industrial organizations. This new technology altogether with polymer nanocomposites has a promising future to become an established manufacturing tool in the design, performance, and implementation of products because of its ability to fabricate geometrically complex parts. But in order for this to happen, polymer nanocomposites with enhanced mechanical, thermal, electrical, and flammability properties that meet commercial requirements have to be developed. Research on this subject matter will continue, and a new technological revolution is promising to happen.

5.2 Future Work

Future work will involve tension testing the remaining of FR/K/NC/MWNT formulations. Once this is done, a formulation from these will be chosen to be compounded in an industrial twin screw extruder to then be cryogenically grinded into fine powder and make SLS test specimens for parameter optimization and testing.

BIBLIOGRAPHY

[1] ISO/ASTM52900-15, "Standard Terminology for Additive Manufacturing - General Principles - Terminology ASTM International West Conshohocken," www.astm.org, PA, 2015.

[2] T. J. Horn, "Overview of Current Additive Manufacturing Technologies and Selected Applications," *Science Progress 95 (3),* pp. 255-282, 2012.

[3] M. S. Wahab, , K. W. Dalgarno, R. F. Cochrane and S. Hassan, "Development of Polymer Nanocomposites for Rapid Prototyping Process," *Proceedings of the World Congress on Engineering (2),* 2009.

[4] J. C. Nelson , J. W. Barlow, J. J. Beaman, H. L. Marcus and D. L. Bourell, "Model of the Selective Laser Sintering of Bishphenol-A Polycarbonate," *Industrial & Engineering Chemistry Research 32 (10),* pp. 2305-2317, 1993.

[5] P. Jain, P. Pandey and P. V. Rao, "Selective Laser Sintering of Clay-reinforced polyamide," *Polymer Composites,* vol. 31, no. 4, pp. 733-738, 2009.

[6] C. Yan, L. Hao, L. Xu and Y. Shi, "Preparation, Characterization and Processing of Carbon fiber/Polyamide-12 Composites for Selective Laser Sintering," *Composites Science and Technology,* vol. 71, no. 16, pp. 1834-1841, 2011.

[7] B. Ong, H. Wu, R. Ortiz, E. Yao and J. H. Koo, "Electrically Conductive Polyamide 11 Nanocomposites for Selective Laser Sintering: Properties Characterization," in *56th AIAA/ASCE/AHS/ASC Structures, Structural Dyanmics, and Materials Conference, AIAA SciTech, (AIAA 2015-1353)*, KIssimmee, Florida, 2015.

[8] J. Manyika, M. Chui, J. Bughin, R. Dobbs, P. Bisson and A. Marrs, "Disruptive technologies: Advances that will transform life, business, and the global economy," May 2013. [Online]. Available: Sustainablebrands.com. [Accessed November 2014].

[9] R. D. Goodridge, C. J. Tuck and R. J. Hague, "Laser Sintering of Polyamides and Other Polymers," *Progress in Materials Science 57 (2),* pp. 229-267, 2012.

[10] S. L. Ford, "Additive Manufacturing Technology: Potential Implications for U.S. Manufacturing Competitiveness," *Journal of International Commerce and Economics,* pp. 1-35, 2014.

[11] S. C. Lao, J. H. Koo, T. J. Moon, B. Hadisujoto, W. Yong, L. Pilato and G. Wissler, "Flammability and Thermal Properties of Polyamide 11-Alumina Nanocomposites," in *Proceedings of the SFF Symposium*, Austin, TX, 2009.

[12] H. Chung, "Processing and Properties of Functionally Graded Polymer Composites Produced by Selective Laser Sintering," *Ph.D, The University of Michigan Ann Arbor,* 2005.

[13] J. H. Koo, S. Lao, W. Ho, K. Nguyen, J. C. Cheng, L. Pilato, G. Wissler and M. Erving, "Polyamide Nanocomposites for Selective Laser Sintering," in *Proceedings of the SFF Symposium* , Austin, TX, 2006.

[14] J. Cheng, S. Lao, K. Nguyen, W. Ho, A. Cummings and J. H. Koo, "SLS Processing Studies of Nylon 11 Nanocoposites," in *Proceedings of the SFF Symposium*, Austin, TX, 2005.

[15] S. C. Lao, M. F. Kan, C. K. Lam, J. H. Koo, T. Koon, M. Londa, T. Takatsuka, E. Kuramoto, G. Wissler, L. Pilato and Z. P. Luo, "Polyamide 11-Carbon Nanotubes Nanocomposites: Processing Morphological, and Property Characterization," in *21st International SFF Symposium - An Additive Manufacturing Conferece*, Austin, TX, 2010.

[16] M. Yuan, B. Johnson, J. H. Koo and D. L. Bourell, "Polyamide 11-MWNT Nanocomposites: Thermal and Electrical Conductivity Measurements," *Journal of Composite Materials,* vol. 48, no. 15, pp. 1833-1841, 2013.

[17] D. Z. Chen, S. C. Lao, J. H. Koo, M. Londa and Z. Alabdullatif, "Powder Processing and Properties Characterization of Polyamide 11-Graphene Nanocomposites for Selective Laser Sintering," in *Proceedings of the SFF Symposium* , Austin, TX, 2010.

[18] S. Gaikwad, J. S. Tate, N. Theodoropoulou and J. H. Koo, "Electrical and Mechanical Properties of PA11 Blended with Nanographene Platelets Using Industrial Twin-Screw Extruder for Selective Laser Sintering," *Journal of Composite Materials 47 (3),* pp. 2973-2986, 2013.

[19] S. Lao, J. H. Koo, A. Morgan, H. Jor, G. Wissler, L. Pilato and Z. P. Luo, "Flammability Intumescent Polyamide 11 Nanocomposites," in *Proceedings of SAMPE*, 2007.

[20] B. Johnson, E. Allcorn, M. G. Baek and J. H. Koo, "Combined Effects of Montmorillonite Clay, Carbon Nanofiber, and Flammability on Mechanical and Flammability Properties of Polyamide 11 Nanocomposites," in *SFF Symposium*, Austin, TX, 2011.

[21] S. C. Lao, C. Wu, T. J. Moon, J. H. Koo, A. Morgan, L. Pilato and G. Wissler, "Flame-Retardant Polyamide 11 and 12 Nanocomposites: Thermal and Flammability Properties," *Journal of Composite Materials 43 (17),* pp. 1803-1818, 2009.

[22] S. C. Lao, J. H. Koo, T. J. Moon, M. Londa, C. C. Ibeh, G. E. Wissler and L. A. Pilato, "Flame-retardant Polyamide 11 Nanocomposites: Further Thermal and Flammability Studies," *Journal of Fire Sciences ,* 2011.

[23] S. C. Lao, W. Yong, K. Nguyen, T. J. Moon, J. H. Koo, L. Pilato and G. Wissler, "Flame-retardant Polyamide 11 and 12 Nanocomposites: Processing, Morphology, and Mechanical Properties," *Journal of Composite Materials 44 (25),* pp. 2933-2951, 2010.

[24] A. Hao, I. Wong, H. Wu, B. Lisco, B. Ong, A. Sallean, S. Butler, M. Londa and J. H. Koo, "Mechanical, Thermal, and Flame-Retardant Performance of Polyamide 11-Halloysite Nanotube Nanocomposites," *Journal of Materials Science 50 (1),* pp. 157-167, 2015.

[25] S. C. Lao, J. H. Koo, T. J. Moon, W. Yong, C. Lam, J. Zhou, B. Haisujoto, G.

Wissler, L. Pilato and Z. P. Luo, "Flame Retardant Intumescent Polyamide 11 Nanocomposites-Further Study," *Journal of Composite Materials ,* vol. 47, no. 923, pp. 2973-2986, 2013.

[26] R. D. Goodridge and M. L. Shofner, "Processing of a Polyamide-12/carbon nanofiber composite by laser sintering," *Polymer Testing,* vol. 30, no. 1, pp. 94-96, 2011.

[27] B. A. Johnson and J. H. Koo, "Analysis of the selective laser sintering process using nanocomposite materials," in *Proceeding of SAMPE*, Covina, CA, 2012.

[28] H. Wu, M. Krifa and J. H. Koo, "Flame Retardant Polyamide 6/Elastomer Blends: Processing and Characterization," in *Proceedings of SAMPE*, Seattle, WA, 2014.

[29] J. H. Koo, Polymer Nanocomposites, New York: McGraw-Hill, 2006.

[30] UL 94, "Test for Flammability of Plastic Materials for Parts in Devices and Appliances," Underwriters Laboratories Inc, Northbrook, Il, 2001.